HZDR-135

EWPAA 2024

EUROPEAN WORKSHOP ON PHOTOCATHODES FOR PARTICLE ACCELERATOR APPLICATIONS 2024

SEPTEMBER 17 – 19, 2024
DRESDEN, GERMANY

Summary of Oral Contributions

Wissenschaftlich-Technische Berichte
HZDR-135 · 2025 · ISSN 2191-8708

WISSENSCHAFTLICH-
TECHNISCHE BERICHTE

HELMHOLTZ ZENTRUM
DRESDEN ROSSENDORF

Wissenschaftlich-Technische Berichte
HZDR-135

EWPAA 2024

EUROPEAN WORKSHOP ON PHOTOCATHODES FOR PARTICLE ACCELERATOR APPLICATIONS 2024

SEPTEMBER 17 – 19, 2024
DRESDEN, GERMANY

Summary of Oral Contributions

Edited by
Rong Xiang, Anton Ryzhov, Lee B. Jones,
Tim C.Q. Noakes, Laura Monaco, Daniele Sertore,
Maud Baylac, Julius Kühn, Romain Ganter

Hosted by
ELBE Department, Institute of Radiation Physics
Helmholtz-Zentrum Dresden – Rossendorf e. V.

HZDR
HELMHOLTZ ZENTRUM
DRESDEN ROSSENDORF

Print edition: ISSN 2191-8708

Electronic edition: ISSN 2191-8716

The electronic edition is published under Creative Commons License (CC BY 4.0):

https://www.hzdr.de/publications/Publ-40942

https://nbn-resolving.org/urn:nbn:de:bsz:d120-qucosa2-956010

2025

Published by

Helmholtz-Zentrum Dresden - Rossendorf

Bautzner Landstraße 400

01328 Dresden

Germany

ELBE.

HZDR
HELMHOLTZ ZENTRUM
DRESDEN ROSSENDORF

EWPAA 2024

European Workshop on Photocathodes for Particle Accelerator Applications

in Dresden

17-19 September 2024

Helmholtz-Zentrum Dresden-Rossendorf
Radiation Source ELBE

Webpage: https://events.hifis.net/e/ewpaa2024

Local contacts: r.xiang@hzdr.de | a.ryzhov@hzdr.de

DRESDEN concept
SCIENCE AND INNOVATION CAMPUS

EWPAA 2024, September 17th - 19th, Helmholtz-Zentrum Dresden-Rossendorf e.V., Dresden

European Workshop on Photocathodes for Particle Accelerator Applications 2024 – Summary of Oral Contributions

R. Xiang[a,*], A. Ryzhov[a,*], L.B Jones[b,c,*], T.C.Q. Noakes[b,c], L. Monaco[d], D. Sertore[d], M. Baylac[e], J. Kühn[f] and R. Ganter[g]

[a] *HZDR, SRF–Gun Group, ELBE Department, Institute of Radiation Physics, Helmholtz–Zentrum Dresden–Rossendorf, 01328 Dresden, Germany*
[b] *ASTeC, STFC Daresbury Laboratory, Warrington, Cheshire, WA4 4AD, UK*
[c] *Cockcroft Institute of Accelerator Science & Technology, WA4 4AD, UK*
[d] *INFN Milano - LASA, Segrate (MI), Italy*
[e] *Univ. Grenoble Alpes, CNRS, Grenoble INP, LPSC-IN2P3, 38000 Grenoble, France*
[f] *HZB, Helmholtz–Zentrum Berlin für Materialien und Energie GmbH, 14109 Berlin, Germany*
[g] *Paul Scherrer Institute PSI, 5232 Villigen PSI, Switzerland*
[*] ***Corresponding Authors:*** *r.xiang@hzdr.de, a.ryzhov@hzdr.de and lee.jones@stfc.ac.uk*

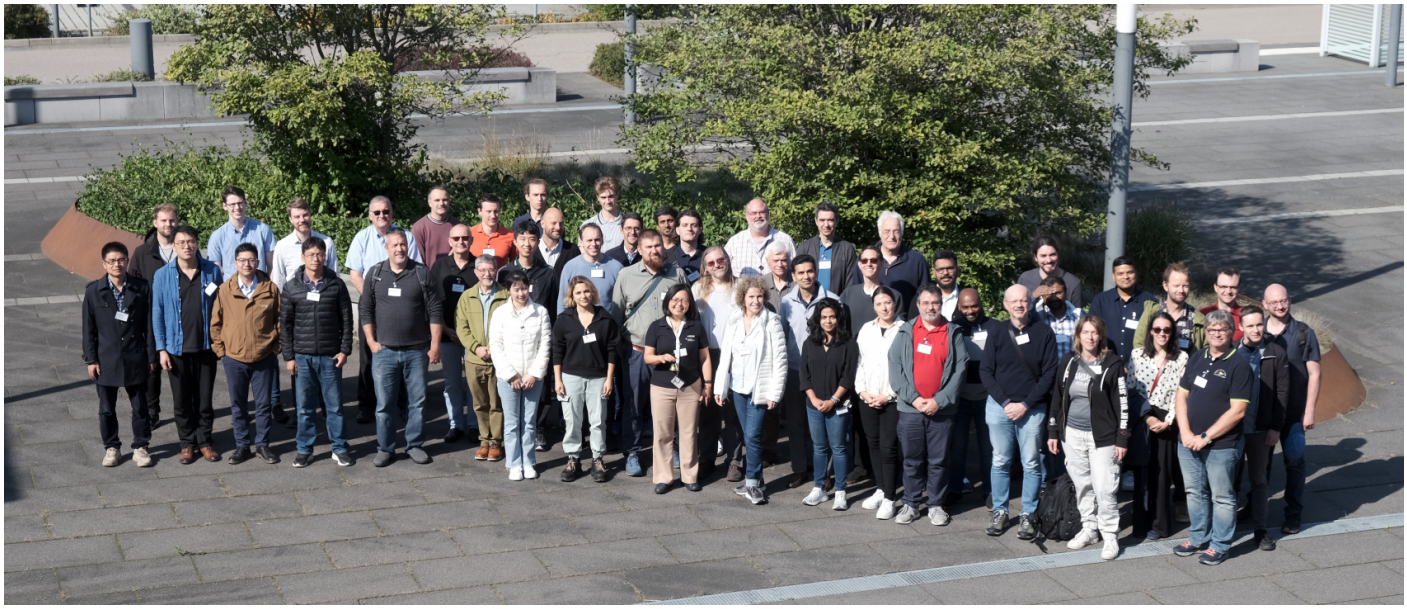

Delegates at the EWPAA 2024 Workshop outside the HZDR facility. In total, 64 participants attended this 2½ day workshop.

The European Workshop on Photocathodes for (particle) Accelerator Applications (EWPAA) brings together experts in the field of photocathode electron sources for use in particle accelerators with the aim of sharing their knowledge and latest research and development progress in this crucial field of particle accelerator science.

The workshop is convened every other year, and is thus complementary to the P^3 workshop (Photocathode Physics for Particle accelerators) run in the USA. Consequently, there is a workshop focusing on photocathodes for particle accelerator applications convened every year, either in Europe or the USA.

The EWPAA 2024 is the 5th meeting in this workshop series. The event was hosted by the ELBE Department at the HZDR Helmholtz–Zentrum Dresden–Rossendorf in Dresden between September 17th and 19th. Photocathodes have been developed, studied and utilized in SRF photoinjectors at the ELBE center for more than 20 years.

The programme was organised with 7 working groups, with each oral contribution assigned to the most appropriate group. Details of the event and the scientific programme can be found at the website https://events.hifis.net/event/1255/overview. The proceedings present the main points raised by each of the speakers in their oral presentations.

The Local Organizer Committee acknowledges the EWPAA Scientific Programme Members for their support in drafting and delivering the agenda and thanks them for their help in organizing and achieving such a successful event.

The organizers also gratefully acknowledge the Deutsche Forschungsgemeinschaft (DFG, German Research Foundation) for their part-funding of the workshop cost under DFG Project No. 545151564.

The next workshop in 2026 will be hosted by the Irène Joliet-Curie Laboratory (IJCLAb) at Orsay in Paris.

Contents

Photocathode Activities in Europe

D. Sertore[a]

[a]*INFN Milano - LASA, Segrate (MI), Italy*

1. Abstract

Activities on photocathodes are constantly evolving. In Europe, in particular, new experiments/accelerators are emerging alongside the historical players in the field. This presentation aims to update the status of activities in Europe from the state made at EWPAA2022, with a focus on new initiatives and emerging topics.

2. Introduction

The present collection presents the latest activities in the field of photocathodes in Europe, since the last EWPAA workshop in Milano. It is a personally driven selection of topics and the author apologize for possible missing items. All the presented work have been selected from recent Conferences (IPAC23, IPAC24, SRF23, 2023-P3) and publications. Due to limited space, the reader is encouraged to refer to the presentation at the Workshop for references.

3. Metallic Photocathodes

Pure copper photocathodes are widely used in many accelerators (ELETTRA, SparcLAB in LNF, CTF2, etc.) as high brightness electron sources, notwithstanding their low Quantum Efficiency (QE). HZDR has used in the past, besides the copper, also Mg as a photocathode.

Study on plasmon excitation on Cu surfaces characterizes the work done at CERN and DESY. At CERN, they have developed a complete work path from simulation, production to experimental validation.

In DESY, they are working on a new Cu plasmon enhanced photocathode for High Duty or CW operation of the E-XFEL injector. At DESY, there also an activity related to field emission from a copper tip in the framework of a half cell RF gun for UED applications.

At UKRI, the approach is to improve either Cu performance by Cs^+ implantation or gold QE by thin Yittria film (of the order of nm's).

Finally, a new activity start in FSU on the study of attosecond emission from tips and laser-tip interaction.

4. Semiconductor Photocathodes

Semiconductor photocathodes have higher QE than metallic one, but their sensitivity to gas pollution requires more stringent vacuum requirements. Typical compounds used in accelerator applications are compound of alkali metals with either tellurium or antimony.

4.1. Alkali Telluride

Cesium telluride is the workhorse of many high brightness electron sources for user applications with high repetition rate or long pulses.

HZDR and SwissFEL at PSI deposit Cs_2Te film on Cu substrate. Both laboratories show long operation lifetime of their photocathodes: SwissFEL, for example, has produced only four photocathodes since 2016. HZDR experience in handling photocathode for SRF guns has triggers a collaboration with MSU for developing the new cathode movement system for the quarter wavelength SRF gun.

At DESY, they have achieved remarkable photocathode lifetime both in FLASH and in E-XFEL. Their photocathodes are now in operation for more than four years providing the electron beam for their user facilities. While vacuum plays a key role in guaranteeing the reported lifetime, only large QE non-uniformity or non-homogeneity determined photocathode exchange.

CERN is also working actively on cesium telluride and, in particular, they are developing their own procedure for cathode rejuvenation. Instead of the UV assisted process, they deposit additional, in sequential mode, cesium and tellurium. This process allowed extending the lifetime of a single cathode to more than 6 years.

Experiments to understand correlation between QE and MTE are performed at UKRI. Poisoning gases as N_2 and O_2 influence the photocathode properties, confirming the activity of oxygen on photocathode performances. Besides basic activity on Cs_2Te, UKRI is also studying RbTe material as photocathode material by implanting Te^+ on Mo and then evaporating Cs, followed by heating cycle to form RbTe. XPS measurements confirm the formation of the telluride compound.

4.2. Alkali Antimonide

PERLE project is a newcomer to the field of alkali antimonide photocathodes. It is a demonstrator for an ERL machine to be installed at IJCLab. The electron source is based on a DC gun and a photocathode preparation system both of them commercial products. Actually, first components are being installed and the experimental hall in preparation.

UniSalerno with Alice Galdi is deeply involved in the developments of alkali antimonide photocathodes, with special interest on epytaxial growths (see CsSb). A strong collaboration with Cornell and Phoebe Lab is at the core of this activity.

HZB focalizes its activity on Na_2KSb photocathodes in preparation for their use in the SRF gun of the SEALab accelerator. Presently, they are involved in moving the photocathode laboratory to a site and in getting all the necessary authorizations. Meanwhile, they have also developed PhoTEx for thermal emittance measurements.

At INFN Milano, a second batch of alkali antimonide photocathodes has been prepared and tested in the RF gun at DESY PITZ. Different materials, namely KCsSb and (Cs)NaKSb were deposited and tested. Preliminary results show that this batch of photocathodes show a significant smaller dark current with respect to the first batch, but yet not as low as for Cs_2Te.

5. Other Photocathodes

5.1. Thermionic laser assisted photoemission

At LINAC2 at ELSA in Bonn a hybrid electron gun is planned that will use a thermionic gun. The electron generation will be possible in a double mode operation: either in the classical mode or as laser assisted photoemission from the heated source.

5.2. Polarized photocathode

At the Photo-CATCH lab in TUD in Darmstad, a study is ongoing for modelling the photocurrent during production in view of an automatization of the process. They achieved good agreement with experimental data by using empirical model.

6. Computational Theory

The Oldenburg University continues its activity on modeling both alkali telluride and antimonide photocathodes and studying their properties by DTF techniques. They have recently added a high-throughput screening calculations based on density-functional theory (DFT) and make it open available. For results are very promising as well as the results obtained on vibrational modes of alkali antimonide photocathodes.

7. Networking

Networking within the European laboratories doing photocathodes is growing, and new laboratories are joining. The relationships between labs are growing too, and a more interactive environment is building up beneficial for the whole community.

Cathode Activities in Asia

Masao Kuriki[a]

[a]*Graduate School of Advanced Science and Engineering, Hiroshima University*

1. Abstract

Photo-cathode is a key technology in advanced accelerator project because the beam property including the helicity can be controlled by the laser. Photo-cathode research activities in Asia are reviewed.

2. GaAs cathode

GaAs cathode has been developed as a source of the spin-polarized electron source. T. Nakanishi initiated the GaAs cathode R&D activity in Asia and the performance was improved by introducing a state-of-the-art crystal technology such as the strained super-lattice structure which realized up to 90% spin polarization limited up to 50% in principle with the bulk GaAs. Strain-compensate super-lattice developed by X. Jin [1] is an advanced form. In the crystal, the strain direction is changed layer by layer. This technique can create the localized strain necessary for high polarization without growing global distortion. It can coexist with high quantum efficiency because many layers can be built up without compromising crystal quality. 90% polarization with 1.5% quantum efficiency were demonstrated simultaneously.

In addition to the spin polarization, another advantage of GaAs is a small thermal energy down to 40 meV [2]. On the other hand, the robustness and the operational lifetime of the cathode are limited. It requires a very high vacuum quality less than 1e-9 Pa and it is compatible only with the DC biased gun. The reason of the limited robustness of the cathode is NEA (Negative Electron Affinity) surface formed by Cs and Oxygen /NF_3 evaporation. There are several studies to improve the robustness and an approach is forming NEA surface by hetero-junction with a thin semiconductor layer. K. Uchida applied Cs and Te to form CsTe layer on GaAs to produce NEA state [3]. Figure 1 shows an example of GaAs quantum efficiency activated with Cs and Te as a function of photon energy. 5 Angstrome Te was applied on the cleaned Zn doped GaAs at RT, 205 Angstrome Cs was applied at 120 deg. C, and Cs was applied again at RT.

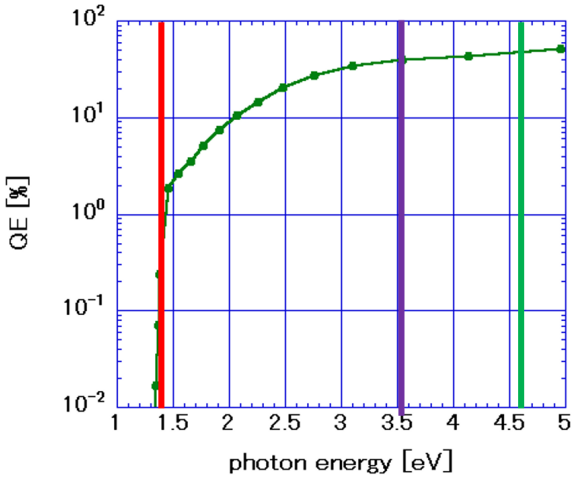

Figure 1. Quantum efficiency of GaAs activated with Cs and Te, as a function of photon energy.

GaAs activation was also confirmed with CsKTe[4]. QE was in order of 10^{-5} at 1.4 eV photon energy, the operational lifetime without beam extraction was confirmed as $(6.50 \pm 0.01) \times 10^{-3}$Pa.sec, which is significantly larger thant that for GaAs activated with Cs and oxygen. By assuming 1.0×10^{-7} in RF Gun cavity, it can be operated 7.7 hours as 1/e life.

GaAs activation with CsSb and oxygen was studied and 0.2% QE was obtained[5].. The evaporation order was 1) Cs, 2) Cs and oxygen co-evaporation, 3) Sb, 4)Cs, and 5) Cs and oxygen co-evaporation.

3. Multi-Alkali cathode

CsK_2Sb cathode has been studied as a robust cathode driven by a green laser. The robustness was analyzed with two components life-times, regarding the product of time and pressure, and the extracted charge density[6]. The temporal and charge density lives were obtained as 4.6×10^{-5}(h.Pa) and $6000 \pm 2000 \pm 2000$ C/mm^2, respetively. These results show a high robustness.

The substrate dependence of the cathode performance was studied for CsK_2Sb cathode [7]. Cleaned and crystalined substrates showed better performance (QE) than the as-received and amorphous substrates for Si(100), Si(111), Mo(100), GaAs(100). Cleaned Si(100) shows 9.4 ± 0.7 %, on the other hand, cleaned Si(111) shows 2.3 ± 0.3 %. The difference can be understood by the crystal atomic arrangement of CsK_2Sb grown on each substrate. By considering atomic arrangement matching, CsK_2Sb is grown in (100) and (111) directions on those crystals with (100) and (111) surfaces, respectively. CsK_2Sb (100) and (111) surfaces correspond to X and L points in the Brilion diagram with 1.4 eV and 3.1 eV band gap energies, respectively. It can be a reson of QE difference.

Compatibility of CsK_2Sb cathode and a superconducting cavity was confirmed with DC-SRF gun[8]. CsK_2Sb was fabricated with 4.3% QE at RT, but it decreased down to 0.3% in DC-SRF gun due to the operation temperature (LN). 150 pC bunch with 1 MHz repetition was confirmed.

4. Graphene coated cathode

Graphene is a 2D crystal of carbon. It is transparent for photons and electrons, but not molecules. H. Yamaguchi proposed that graphene as a protective layer on the cathode preventing chemical poisoning. The photo-cathode covered by the graphene was formed as follows. 2 layers of graphene are formed on a Ni mesh with a 60% aperture ratio. The photocathode (CsK_2Sb)is formed on the graphene (other side of Ni mesh) and caped by Ni layer by evaporation. By illuminating 3.4 eV UV light on the cathode through graphene, 0.17% QE was confirmed[9]. The 1/e lifetime was 188 hours with an 8.6 nA average current. That was the first observation of the electron emission from the graphene-coated cathode. The protective performance of the graphene coating was evaluated by measuring QE under a continuously increasing pressure environment. Without the protection, QE was dropped at the pressure in the order of 10^{-7}Pa. With the protection, QE was kept up to 1×10^{-3}Pa. The same measurement was performed with Cu cathode and the result was same. That suggests that the bi-alkali cathode coated with the graphene has a high robustness same as Cu cathode. The graphene is also good as a substrate of an evaporation cathode. The graphene is a promising reusable substrate, as photo-cathodes deposited on it maintained stable quantum efficiency (QE) after multiple thermal cleanings, unlike those on Si and Mo[10].

[1] X. Jin, *et al.* ; Appl. Phys. Lett. **105**, 203509 (2014)
[2] N. Yamamoto, *et al.* ; J. Appl. Phys. **102**024904 (2007)
[3] K. Uchida, M. Kuriki, *et al.*; Proc. of IPAC2014, MOPRI032(2014)
[4] M. Kuriki and K. Masaki; J. Phys.: Conf. Ser. 1350,012047 (2019)
[5] Y. Wakita, L. Guo, Y. Takashima, M. Kuriki; *Proc. of IPAC24*,WEPC62 (2024)
[6] M. Kuriki, A. Yokota, *et al.*; *Proc. of LINAC16*:TUPLR013 (2016)
[7] L. Guo, M. Kuriki *et al.*;*Prog. Theor. Exp. Phys.* 033G01(2017)
[8] D. Ouyang, H. Xie, *et al.*;*NIMA***1026**166204(2022)
[9] L. Guo, H. Yamaguchi, *et al.*;*Sci. Rep.***13**2412(2023)
[10] L. Guo *et al.*;*Appl. Phys. Lett.***116**251903(2020)

Photocathodes for High Brilliant Electron Beams

Chen Wang[a,b], **Julius Kühn**[a], **Jonas Dube**[a,c] **and Thorsten Kamps**[a,c]

[a] *Department of High Brightness Beams, HZB, Berlin, Germany*
[b] *University of Siegen, Siegen, Germany*
[c] *Humboldt University of Berlin, Department of Physics, Berlin, Germany*

1. Abstract

The goal of the Sealab / bERLinPro project is to build a new generation superconducting RF electron accelerator at HZB. Na-K-Sb photocathode deposited on Mo plug is chosen for this application for its high QE at green laser, long dark lifetime and high thermal stability. Currently, Na-K-Sb photocathodes are produced in UHV preparation chamber at photocathode lab. In the contribution, we will present our experience for film growth (2 recipes), as well as the QE, dark lifetime and thermal stability on Na-K-Sb photocathodes. Besides, we would also like to give an introduction of the update of preparation system at photocathode lab.

2. Experimental Setup

In the photocathode lab, a series of Na-K-Sb photocathodes are grown and analyzed in the UHV-chamber, which was designed for producing photocathodes for the Sealab facility at HZB[1]. Photocurrent can be measured in situ and chemical composition is analyzed by XPS.

3. Growth Methods

Two growth recipes for Na-K-Sb film are developed at photocathode lab. The first recipe is modified alkali sequential growth. In first step, K is deposit on 40 nm Sb layer for K_3Sb film, which can achieve approximately 0.1 % to 0.3 % quantum efficiency (QE) at 515 nm. Then the sample is raised to approximately 150 °C for Na deposition without turning off the K dispensers to minimize the loss of K at elevated temperatures. The photocurrent starts to increase, and once it reaches plateau, the Na dispensers need to be turned off immediately to avoid Na saturation.

The second recipe is alkali co-deposition method to simplify the growth process. After Sb deposition, we directly heat the sample to 150 °C and activate both K dispensers and Na dispensers with a higher flow rate for K than Na. The photocurrent begins to increase and turn off both dispensers once photocurrent reaches plateau.

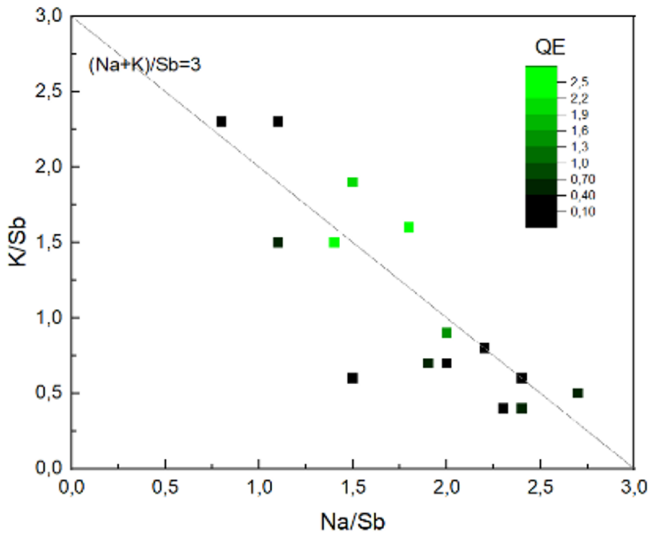

Figure 1. Quantum efficiency and chemical composition of Na-K-Sb photocathodes.

4. Composition of Na-K-Sb Photocathodes

After film deposition, Na-K-Sb photocathode sample will be transferred to analysis chamber to determine its chemical composition by XPS. The stoichiometry of 15 Na-K-Sb is shown in figure 1. X-axis and y-axis represent the chemical composition, the line of $(Na + K) / Sb = 3$ represents Sb is almost fully reacted with alkalis.

We can conclude that a qualified Na-K-Sb photocathode (with QE higher than 1.0 %) needs to fulfill 2 requirements:

1. Alkali sufficient, the ratio between alkali to Sb needs to close to or higher than 3;
2. K/Sb ratio is between 1.0 to 2.0;
3. When K/Sb is close to 1.5, QE is the highest, approximately 2.5 %.

5. Dark Lifetime of Na-K-Sb Photocathodes

Table 1. Dark lifetime of Na-K-Sb and Cs-K-Sb photocathodes.

Type	Number	QE (max) at 515 nm	XPS stoichiometry			Days >1.0%
			Na/Sb	K/Sb	Alkali/Sb	
Na-K-Sb	WH09	2.6%	1.4	1.5	2.9	++
	WH14	2.4%	1.8	1.6	3.4	++
	WH17	1.9%	1.5	1.9	3.4	16
Cs-K-Sb	P16	4.8%	-	-	-	5
	P18	3.4%	-	-	-	11

As shown in table 1, dark lifetime of Na-K-Sb photocathodes is measured in the preparation chamber after XPS measurement, the pressure is kept at low 10^{-10} mbar. Generally, the dark lifetime of Na-K-Sb film is much higher than Cs-K-Sb. Especially for WH09 and WH14, the decay of QE is relative slight (< 20 %) in the period of measurement time (2-3 weeks), when K to Sb ratio close to 1.5. Higher K composition seems to result in the decrease of dark lifetime for WH17, but still higher than Cs-K-Sb (P16, P18).

In thermal stability test of WH09, it can remain 1.2 % QE at 100 °C, which is 60 % of its QE at room temperature, the figure is shown in presentation

6. Outlook and Future Work

The preparation chamber of Na-K-Sb is upgraded, which allow triple evaporation of Sb, Na and K. The alkali source is upgrade from dispensers to effusion cells filled with alkali pills (Alkali /AMAX/PILL/6-3), which allow us to deposit multiple films without change alkali source.

Synchrotron radiation study of Na-K-Sb will be conducted at EMIL in October to measure the homogeneity (in depth XPS), chemical surrounding (XAS) and valence band of Na-K-Sb films.

In October or November, a photocathode will be provided to the operation of Sealab facility. QE, beam emittance and operational lifetime will be tested in situ.

[1] Schmeißer, Martin A.H. *et al.*; Phys. Rev. Accel. Beams **21**, 113401 (2018)

Cathode for mA high current

Huamu XIE

State Key Laboratory of Nuclear Physics and Technology, Peking University, Beijing, China

1. Abstract

High-brightness electron sources are crucial for applications like X-ray free electron lasers (XFEL), ultrafast electron diffraction (UED), and electron ion colliders (EIC), etc. At Peking University, the DC-SRF gun operates reliably at a low emittance mode of 0.54 mm·mrad(normalized) with 100 pC bunch charge at 1 MHz repetition rate, and a high current mode of 37 pC at 81.25 MHz (3 mA). The K-Cs-Sb photocathode is illuminated by a 515 nm green laser, achieving a quantum efficiency (QE) of 6-8%, which drops to around 1% in the cold gun electrode at 30 K. The photocathode maintains its QE for up to a month during experiments, delivering 0.1-3 mA during up to 16-hour continuous-wave (CW) test. Additionally, the intrinsic emittance of the bialkali photocathode was also evaluated.

2. Experiment results

In the first section, the fabrication and transport of a K-Cs-Sb photocathode at Peking University are introduced. More than 5 percent quantum efficiency (QE) bialkali photocathodes have been routinely produced at PKU. The transport of the photocathode from the deposition system to the gun is well-established, and the QE shows no decay during the transport process. Beam experiments are conducted with different photocathodes and varying milliamperage (mA) levels of the K-Cs-Sb photocathode in the DC-SRF gun. An average current of 0.1 mA is maintained for more than 16 hours, and peak average currents of up to 3 mA can be achieved from the DC-SRF gun. During the beam experiments, the lifetime of the photocathode is greatly influenced by the vacuum conditions of the gun, as shown in Table 1 in section 3.2. Additionally, the intrinsic emittance of the bialkali photocathode is measured in the lab.

3. Figures and Tables

3.1. Figures

The CW operation of the beam has been successfully accomplished with a bunch charge of 100 pC and a repetition rate of 1 MHz. The beam experiment has continued for over 16 hours, during which an emittance of 0.54 mm·mrad was measured at the exit of the DC-SRF gun (refer to the paper arXiv:2406.00659).

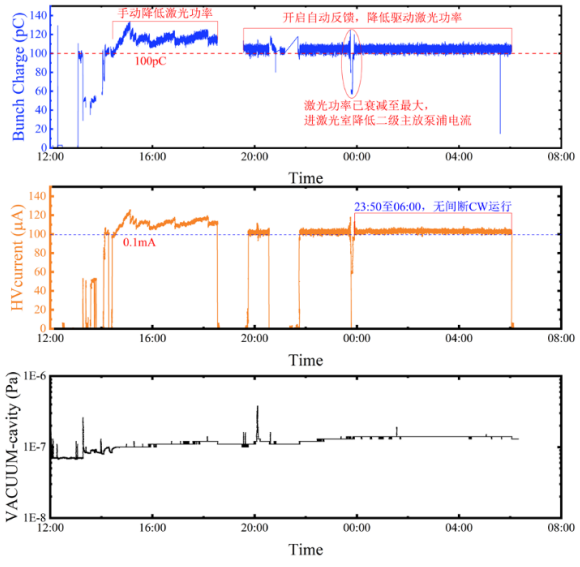

Figure 1. CW operation of the photocathode at 0.1 mA

The mA-level CW beam extraction was achieved at a repetition rate of 81.25 MHz, with the quantum efficiency (QE) demonstrating no significant decay during operation. A feedback control loop has been integrated into the laser to maintain a stable bunch charge.

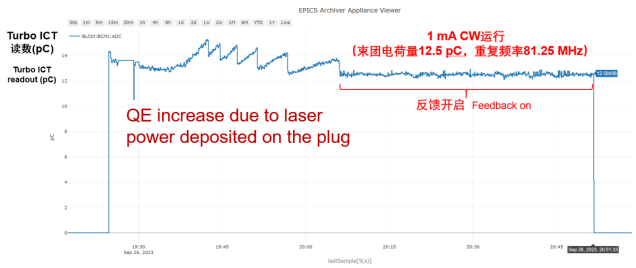

Figure 2. CW operation of the photocathode at 1 mA

A continuous wave (CW) average current of 2 to 3 mA (12 to 40 pC at a repetition rate of 81.25 MHz) has been achieved in the DC-SRF-II gun. The operation at 2 mA and 3 mA utilized a 3 mm laser spot, resulting in total extraction charges of 1.4 C and 0.9 C, respectively.

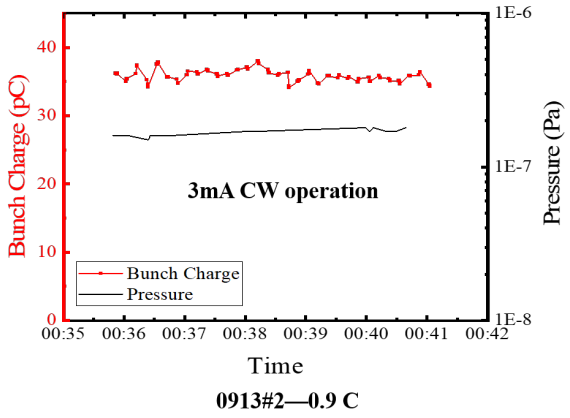

Figure 3. CW operation of the photocathode at 3 mA

3.2. Tables

Table 1 shows the average lifetime of the K-Cs-Sb photocathode in the DC-SRF gun is significantly affected by the vacuum conditions of the gun. For optimal performance, the typical vacuum level for the K-Cs-Sb photocathode should be in the low -8 Pa range.

Table 1. The lifetime of K-Cs-Sb photocathode at different vacuum

Commis. time	Pressure/Pa	Lifetime/Days
2023.03.31-2023.06.28	2E-6	3
2023.08.28-2023.09.28	8E-8	7
2023.12.29-2024.02.06	3E-8	20

4. Outlook and Future Work

The beam experiment in the DC-SRF gun will aim for an average current of 6-8 mA this year. The intrinsic emittance of the bialkali photocathode at RT and cryogenic temperatures in the DC-SRF gun will be measured further.

Boosting Photocathode Performance through Plasmonic Effects and In-situ Rejuvenation Techniques

E. Granados[a], M. Martinez-Calderon[a], B. Groussin[a], L. B. Jones[b,c], P. Katona[a], E. Chevallay[a] and R. E. Rossel[a]

[a] *CERN, European Organization for Nuclear Research, 1211 Geneva, Switzerland*
[b] *ASTeC, STFC Daresbury Laboratory, Warrington, United Kingdom*
[c] *Cockcroft Institute of Accelerator Science, Daresbury, United Kingdom*

1. Abstract

Semiconductor Cs-Te photocathodes are essential components in high-brightness electron sources, playing a pivotal role in the operation of large-scale accelerators. However, their operational lifetime and efficiency remain critical challenges. To address these challenges, we explore two complementary approaches to enhance photocathode performance and longevity: First, we analyze the systematic production and rejuvenation of Cs-Te photocathodes, and second, we introduce a novel method to overcome the limitations of conventional photocathodes by utilizing direct-laser nanostructuring techniques on copper substrates. This nanoengineering approach excites localized surface plasmons, generating hot electrons that contribute to a substantial increase in quantum efficiency (QE).

2. In-situ rejuvenation of Cs-Te photocathodes

The primary factors contributing to QE degradation include electrical breakdowns, contamination from oxygen and other chemical species (primarily CO_2 and H_2O), and laser-induced damage to the thin-film. When Cs-Te thin-films degrade, they typically require in-vacuum replacement, which can lead to operational interruptions for an accelerator complex. An alternative to replacing the photocathode is rejuvenation, a process that has been relatively understudied but offers a potential means to extend the operational lifespan of the accelerator.

Over the past seven years, we have tested *in-situ* rejuvenation (at the gun level) at the CLEAR facility at CERN. The photoinjector here is equipped with an independent vacuum section behind the gun, which can be isolated. This dedicated chamber contains Cs and Te dispensers. The initial QE of 7.5% gradually declined to 0.5% after nearly three years of operation. Typically, each rejuvenated cathode delivers an integrated charge of up to 1 Coulomb over thousands of hours of use. When the first rejuvenation was performed, it was possible to restore the QE to 4%, which then decayed back to approximately 0.5% after one year of intense use. Similar patterns have been observed in subsequent years, up to the present day, where the CLEAR facility operates 24/7 with minimal photocathode exchange interventions[1].

3. Laser fabricated plasmonic photocathodes

Another alternative relies on the use of plasmonic effects to boost the performance of photocathodes. Here, we propose to enhance the electron photoemission via plasmonically excited hot-electrons in laser-fabricated nanostructures. Plasmonic resonances under DUV laser irradiation require nanofeatures much shorter than the excitation wavelength and in the sub-100 nm scale. The overall quantum efficiency achievable has multiple dependencies, among the most important ones we consider the quality factor of the plasmonic resonance (and consequent hot electron production probability), and the photonic absorption cross-section of the nanostructures based on Mie scattering, which is often close to the wavelength in use. It is challenging to simultaneously optimize both effects with the same type of nanostructure morphology and spatial distribution, and some approaches trade-off between nanostructure size and structure interspacing for optimized photon absorption and plasmonic resonance at the wavelength of interest[2].

We conducted a series of electromagnetic simulations to understand the potential field enhancement of laser-produced nanoparticles under DUV illumination. Figure 1a shows the computed maximum field enhancement $\max\{\beta(r_0,\theta,\rho)\}$ over the nanoparticle surface for a range of radius r at 266 nm illumination. Experimentally, we tested several nanostructured photocathodes with particle sizes in the 30 - 50 nm range. The measurements of the charge generated as a function of laser pulse energy are depicted in Figure 1b, showing significant QE enhancement factors between 5 and up to 25[3].

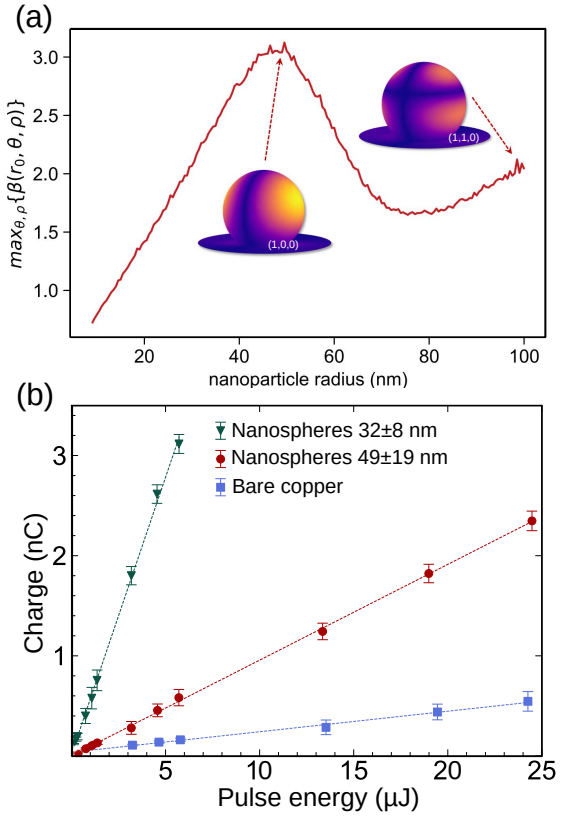

Figure 1. (a) Maximum field enhancement $\max\{\beta(r_0,\theta,\rho)\}$ as function of copper nanoparticle radius r with a penetration depth $h = 0.8r$ under 266 nm illumination. Insets show 3D visualizations of copper nanoparticles of $r = 50$ nm and $r = 100$ nm. (b) Experimental measurements of the charge generated as a function of the delivered UV pulse energy at the center of the nanostructured photocathodes with various nanosphere radii.

4. Outlook and Future Work

Further experiments with optimized semiconductor layers over the nanostructures should be performed to fully understand the potential of combining both techniques, including measurements of the photocathode lifetime, produced electron beam emittance and mean transverse energy among others.

[1] M. Martinez-Calderon *et al.*; Phys. Rev. Acc. Beams; **27** 023401 (2024)

[2] A. Polyakov *et al.*; Sci. Rep.; **2** (1): 933 (2012)

[3] M. Martinez-Calderon *et al.*; Nanophotonics; **13** (11): 1975-1983 (2024)

Overview Of The SwissFEL Photocathode Lasers And Cathode R&D

Alexandre Trisorio[a]

[a] *Paul Scherrer Institute, Villigen - Switzerland*

1. Abstract

SwissFEL, the Swiss Free Electron Laser facility in user operation since 2019 is a 700 m long X-ray FEL delivering femtosecond soft and hard X-ray photons in two parallel beamlines, respectively Athos and Aramis. In order to achieve low emittance and short electron bunches, SwissFEL uses a photo-injector. In that context, the photocathode lasers facility is a crucial subsystem that must seed the photo-electron gun with high-end performance, shaping capabilities as well as long term stability and reliability. In parallel, we produced and used CsTe cathode with high QE and long lifetime. The talk will lead you through the key steps as well as the state of the art technological and optical solutions that have been developed and implemented to build the photocathode lasers facility and the cathode.

2. The Photocathode Lasers Facility

The dual-photocathode lasers (PCDL) architecture developed over recent years at SwissFEL makes use of two compact, industrial-grade, ytterbium laser oscillators and amplifiers ensuring stable, reliable, and cost-effective operation[1]. Thanks to low-cost pump diodes emitting at 980 nm this technological approach is a compelling alternative to the well-established yet more expensive Ti:sapphire (Ti:Sa) laser technology which is widely used at other FEL facilities to the present.

To seed the two FEL lines, the PCDL must deliver two deep-UV pulses separated by 28 ns in order to seed the hard and soft X-ray lines of the FEL. The deep-UV pulse duration, energy, and temporal shape must be independently adjustable for each line. The Laser Heater (LH) and Short Probe (SP) pulses must be available as well. These requirements are fulfilled by using a second PCDL system as in the optical setup depicted in Figure 1. In order to produce a low-emittance electron beam, the PCDL must have a spatially flat-top intensity profile on the cathode plane.

This is a very challenging issue, especially in the UV where both the non-linear conversion stages used to generate the UV radiation and the transport of the laser from the gun laser table down to the cathode (25 m) introduce distortions and high-frequency modulations on the UV beam profile. In order to obtain a circular and smooth beam profile after the transport, we use Fourier filtering in conjunction with aperture clipping of the beam. Moreover, the PCDL must deliver a pair of picosecond, temporally shaped pulses to generate the photoelectrons at the cathode. The temporal pulse shape is programmable between Gaussian (with continuously adjustable duration between 3.3 and 10 ps FWHM) and flat-top (with two distinct durations of 3.7 and 10 ps FWHM). The flat-top pulses are especially desirable for lowering the electron beam emittance, especially at low charge operation of the FEL.

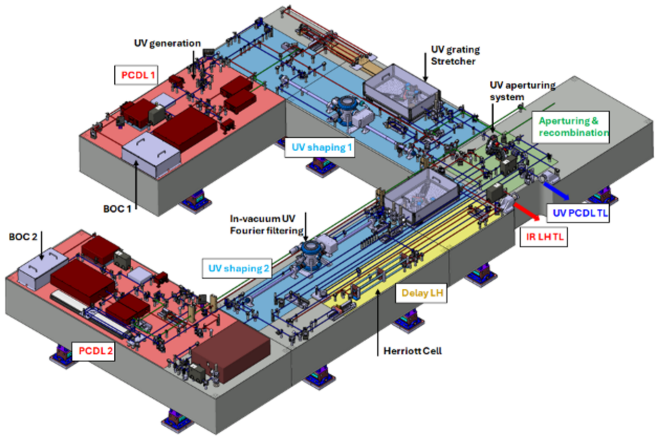

Figure 1. 3D CAD layout of the SwissFEL dual-photocathode drive laser (PCDL) optical setup. The PCDLs 1 and 2 (red areas) are capable of delivering the temporally and spatially shaped, deep-UV pulses (blue areas and green area) as well as the laser heater (LH) and the short probe (SP) pulses for the two free electron laser (FEL) lines. The two UV-PCDLs and the two LH beams are recombined (green area) and sent towards the accelerator via two dedicated imaging transfer lines (TLs). The yellow area includes the LH Herriott cell used to delay the two LH pulses.

3. CsTe Cathodes

We produced our cathode using co-evaporation of Cs and Te compound on a copper cathode plug in a deposition chamber. The cathodes appeared to have a long life-time of 2 years, as well as high QE at 260 nm ranging from 1.3 % down to 0.3 % at the end of the cathode life-time

4. Outlook

The innovative dual-photocathode laser scheme that has been developed at SwissFEL is based on state-of-the-art ytterbium femtosecond laser systems that have proven to be extremely reliable, with a fractional operational readiness of more than 99 % over the past 3 years. The pulse-to-pulse optical performance, timing jitter, and overall stability of the SwissFEL PCDLs are excellent, enabling efficient development of advanced modes of operation. Deep-UV pulse-shaping techniques are successfully implemented to generate temporally tailored Gaussian or flat-top PCDL pulses with variable duration and a flat-top spatial intensity profile. The dual-PCDL architecture was exploited for parallel generation of two electron bunches separated in time by 28 ns with independently controlled properties. Finally the home-made CsTe cathodes appeared to be efficient and have a life time long enough to ensure smooth FEL operation

[1] S. Bettoni, A. Cavalieri, A. Dax, E. Divall, C. P. Hauri, S. Hunziker, M. Huppert, M. Kaiser, M. Paraliev, C. Sydlo, C. Vicario & A. Trisorio; *Overview of SwissFEL dual-photocathode laser capabilities and perspectives for exotic FEL modes*; High Power Laser Science and Engineering (**9**) e51 (2021)

Laser-Plasma Based Electron Sources for FEL Applications

Arie Irman[a]

[a]*Helmholtz-Zentrum Dresden-Rossendorf, Germany*

1. Abstract

Modern laser-wakefield electron accelerators (LWFAs) are capable of generating competitive relativistic electron beams in a compact footprint. For applications such as free-electron lasers, further research on improving the beam quality, stability and system reliability is still required and represents a very active topic as there have been many novel electron injection and acceleration schemes proposed in the last ten years. In this proceeding we briefly report on two promising injection schemes, namely self-truncated ionization injection (STII) for high charge beam and plasma photocathode (PPc) for low emittance beam generation.

2. Introduction

In laser-plasma based electron acceleration[1], an ultrashort high intensity laser pulse is sent into a transparent plasma to excite micrometer-scale cavity-like structure that travels trailing the laser driver at speed close to the light speed. Inside such a cavity, a very strong accelerating field of the order of a few hundred GV/m exists and can be utilized to rapidly boost electron energy from zero to relativistic energies in short distances. To generate electron beams of high quality, electrons have to be injected instantaneously in a specific accelerating phase which is then followed by steady acceleration. As the required spatio-temporal precision for these processes is very stringent, progress in the last decade is linked to proposals and demonstrations of advanced injection techniques, for examples density down-ramp injection, colliding pulse or external injection. Such a compact accelerator now features electron bunches with improved parameters at energies up to 10 GeV, emittances down to 0.1 mm mrad, sub-percent energy spread and nano-coulomb charges with duration typically around 10 fs and sustaining peak currents of kiloamperes.

2.1. Self-Truncated Ionization Injection

In self-truncated ionization injection (STII), electrons from outer shells of a low-Z gas atom are ionized at the up-rising intensity edge of the laser driver to create a well-defined acceleration medium and meanwhile electrons from the K-shell of a high-Z gas atom are released a bit later close to the high intensity location of the laser driver, i.e inside the cavity at the front side. Those electrons are trapped at the cavity rare-side and the injection process is terminated as the laser driver evolves during propagation through the gas target. This results to a narrow energy spread electron beam. The amount of charge can be tuned by adjusting the percentage of high-Z gas composition. As the injection volume and acceleration distance are kept constant, the amount of charge and final electron energy as well as its bandwidth are correlated by the so-called beam loading effect. This way electron beam charge of up-to nC can be generated with a narrow relative energy spread of a few tens of percent.

Beside the capability to generate high charge beams, this regime demonstrates better beam stability. In combination they resembled key components to enable the proof-of-principle experiment of free-electron lasing in a seeded configuration[2]. Together with other FEL lasing results[3,4], these results landmark the development of plasma-based electron accelerators.

2.2. Plasma photocathode

Similar with STII, plasma photocathode (PPc) injection relies on selective ionization in a mixture gas of low and high ionization threshold atoms. Here a dedicated injector laser is deployed at an intensity just above a specific ionization level to release electrons with low residual transverse momentum. The arrival time of the injector laser is tuned such that the injection point is at the cavity center, i.e the longitudinal and transverse fields are zero, decoupled the injection rate from wakefield excitation. This scheme promises better injection control for the generation of background-free ultra-low emittance beams of a few nm.

In order this injection scheme to work, the plasma target needs to be partially ionized. Consequently, the use of high intensity laser pulse driver has to be avoided since it can fully ionize the plasma. Instead the wakefield will be driven by a relativistic electron beam in particle-wakefield acceleration (PWFA) configuration. The drawback of this setup, that traditionally those electron beams are produced in RF-linear accelerators, which is typically required a large infrastructure. As an alternative, we have been working in a hybrid concept, where the high charge electron beams are first generated in a LWFA stage then use it to drive a plasma wakefield in a subsequent plasma module. Because the duration of electron beam driver is very short, thus high peak current, this beam can excite wakefield efficiently in the high plasma density regime, i.e. 10^{18} cm^{-3}. This concept will allow PWFA research in a compact platform, complementing RF-driven PWFA facilities.

3. Status and Outlook

Using 150 TW Draco, a laser system based on chirped-pulse amplification technique using Ti:Sapphire crystals as gain media operated in Helmholtz-Zentrum Dresden-Rossendorf, a stable operation of LWFA at this high charge regime has been established. Upgrading to PW power level, the generated electron beams of very high charge are envisioned to further advance the research on FEL, aiming for EUV radiation. In parallel, plasma photocathode injection is being mastered in a hybrid laser plasma wakefield acceleration platform. Several injection configurations, i.e 90° geometry, counter-and co-propagating injector laser, will be tested. The beam emittance will be measured using several techniques.

[1] Tajima & Dawson; Phys. Rev. Lett. **43**, 267 (1979)
[2] Labat *et al.*; Nat. Photonics **17**, 150-156 (2023)
[3] Pompili *et al.*; Nature **605**, 659-662 (2022)
[4] Wang *et al.*; Nature **595**, 516-520 (2021)

Novel Plasmonic and Photonics Integrated Photocathodes

Alimohammed Kachwala[a] **and Siddharth Karkare**[a]

[a]*Arizona State University, Tempe, AZ, USA*

1. Abstract

Next-generation electron sources, including novel plasmonic and photonics-integrated cathodes, are poised to revolutionize applications ranging from low bunch charge stroboscopic ultrafast electron diffraction and microscopy to beam-driven wakefield accelerators requiring transversely shaped electron bunches. In this study, we report the generation of a record low root mean square (RMS) normalized transverse electron emittance of less than 40 pm-rad from a plasmonic photocathode—a reduction of at least an order of magnitude from previous benchmarks. This was achieved through plasmonic light focusing using Archimedean spiral structures, resulting in an RMS electron emission spot size of approximately 50 nm. Additionally, we demonstrate the feasibility of photonics-integrated photocathodes by utilizing nanofabricated waveguides and thin alkali antimonide photoemissive films to produce transversely shaped electron beams. These findings underscore the potential of these advanced cathodes in developing next-generation high-brightness electron sources for a wide range of accelerator applications.

2. Introduction

Next-generation electron sources, particularly those integrating advanced plasmonic and photonic technologies, are set to revolutionize a range of scientific and technological applications. These sources are crucial for ultrafast electron diffraction and microscopy (UED/M) as well as beam-driven wakefield accelerators that require precise, transversely shaped electron bunches. The demand for higher brightness and lower emittance beams has spurred significant research into novel cathode technologies.

In this study, we report a major breakthrough with a plasmonic photocathode, achieving a record low RMS normalized transverse electron emittance of less than 40 pm-rad—a reduction of at least an order of magnitude from previous benchmarks. This was accomplished using an Archimedean spiral structure to focus light into a nanoscale emission area, reducing the RMS electron emission spot size to approximately 50 nm and significantly enhancing beam coherence and brightness.

Additionally, we demonstrate the potential of photonics-integrated cathodes. By combining nanofabricated waveguides with thin alkali antimonide films, we achieved transversely shaped electron beams, highlighting the versatility of these advanced cathodes. Unlike traditional beam shaping methods that result in significant current loss, our approach allows for efficient nanoscale shaping directly at the cathode surface, offering a scalable solution for advanced accelerator applications.

3. Experimental Section

3.1. Plasmonic Archimedean Spiral Photocathode

Fig. 1 (a) illustrates the experimental setup, where a gold Archimedean spiral plasmonic (ASP) structure is illuminated by a circularly polarized laser with a 150 fs pulse duration and an 800 nm central wavelength. The red waves in the sketch represent the excited surface plasmon polaritons, which constructively interfere at the spiral's center, enhancing the intensity. The inset of Fig. 1 (a) shows a scanning electron microscope image of the fabricated spiral. Fig. 1(b) displays the spatial distribution of the non-linear electron emission spot size, measured using a photoemission electron microscope (PEEM). The rms emission spot size is ∼50 nm, with a mean transverse energy of ∼500 meV it results in a normalized transverse emittance of 40 pm-rad [1].

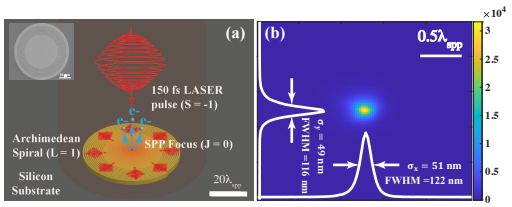

Figure 1. (a) Schematic of a gold Archimedean spiral photocathode illuminated by a circularly polarized laser pulse. (b) Emission profile of electrons measured from the center of the ASP using a PEEM. Here, $\lambda_{spp} = 783$ nm.

3.2. Photonics Integrated Photocathode

The mechanism uses a grating coupler on the surface of the cathode with the laser incident at large angles with respect to the normal as shown in Fig. 2 (a). The grating coupler was designed to couple light at an angle of 65° w.r.t the normal at 532 nm wavelength.

Fig. 2 (b) shows the schematic of Si_3N_4 waveguide. A ∼5 nm thick Cs_3Sb film was grown on the sample. To couple light into the waveguide, it was made incident on the grating coupler. Fig. 2 (c) shows a PEEM image demonstrating that the emission is confined only to regions of the Cs_3Sb photocathode layer over the Si_3N_4 waveguide for coupling wavelength $\lambda = 532$ nm. The transverse patterns in the electron emission are formed due to interference between these co-propagating modes within the waveguide[2]. We have demonstrated a transverse spatial resolution for patterning better than 350 nm using 1 μm wide waveguides.

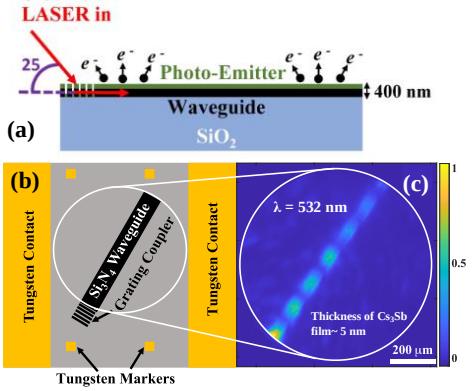

Figure 2. (a) Cross sectional view of light coupling into the waveguide using grating coupler. (b) Schematic of the fabricated sample and (c) first PEEM image showing confined emission from a ∼5 nm thick film of Cs_3Sb photoemitting film for coupling wavelength $\lambda = 532$ nm.

4. Conclusion

In conclusion, integrating plasmonic and photonic elements into electron source design represents a significant advancement in developing ultra-bright, low-emittance electron beams. The breakthroughs reported here set new performance records and open up new research avenues in accelerator science and related fields. As these technologies mature, they are poised to drive significant advancements in both fundamental physics and applied technologies, ushering in a new era of scientific discovery and innovation.

[1] A. Kachwala et al., arXiv preprint; **arXiv:2406.08678 (2024)**
[2] A. Kachwala et al., IPAC2023; **pp. 2178-2181 (2023)**

The Relativistic Ultrafast Electron Diffraction and Imaging (RUEDI) Facility

T.C.Q. Noakes[a], J.W. McKenzie[a], A.R. Bainbridge [a], R.K. Buckley[a], J.A. Clarke[a], L.S. Cowie [a], G. Cox[a], J. Crone[a], M.J. Ellis[a], A. Farricker[a], A.J. Gilfellon[a], M. Hancock[a], C. Hill[a], P. Hornickel[a], B.R. Hounsel[a], J.K. Jones[a], N.Y. Joshi[a], M. King[a], B.L. Militsyn[a], B.D. Muratori[a], T.H. Pacey[a], S.S. Percival[a], L.R. Reid[a], M.D. Roper [a], Y.M. Saveliev[a], B.J.A. Shepherd[a], C. Tollervey[a], A.J. Vick[a], A.E. Wheelhouse[a], J. Wilson[a], F. Yaman[a], N.D. Browning[b], Y. Murooka[b], M. Patel[b] and A.I. Kirkland[c]

[a] *STFC Daresbury Laboratory and Cockcroft Institute, Sci-Tech Daresbury, Warrington, UK*
[b] *School of Engineering, University of Liverpool, Liverpool, UK*
[c] *Rosalind Franklin Institute, Rutherford Appleton Laboratory, Harwell Campus, Didcot, UK*

1. Abstract

The Relativistic Ultrafast Electron Diffraction and Imaging (RUEDI) facility has been recently approved by the UKRI Infrastructure Fund to be a new ultrafast science capability for the UK based at Daresbury Laboratory. It will deliver single-shot, time-resolved, imaging with MeV electrons, and ultrafast electron diffraction down to 10 fs timescales. RUEDI is being designed to enable the following science themes: dynamics of chemical change; materials in extreme conditions; quantum materials; energy generation, storage, and conversion; and biosciences. The evolution of the design of the facility will be outlined along with the remaining challenges to deliver a world leading capability. Particular reference to the photoinjector and photocathode options chosen will be made.

2. Introduction

The RUEDI project is led by the University of Liverpool with the Rosalind Franklin Institute and STFC Daresbury Laboratory as the other main partners. It aims to establish a UK national facility for ultrafast electron diffraction and imaging. Five main science themes have been identified; dynamics of chemical change; materials in extreme conditions; quantum materials; energy generation, storage, and conversion; and biosciences.

3. RUEDI Design

The RUEDI design has evolved significantly from the initial concept of a single beamline for both techniques to two separate lines but with some shared laser and RF infrastructure.

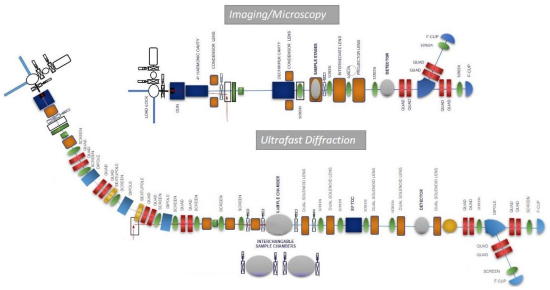

Figure 1. Current RUEDI Beamline designs.

3.1. Diffraction Line

The electron source for the diffraction line will be a 2.4 cell S-band RF photoinjector with side coupling of RF, $\beta = 2$ and a stepped power profile to facilitate fast filling which will minimise dark current. The gun will have a solid copper rear wall that will act as the photocathode to avoid the additional dark current emitted from the puck and backplate rims with an interchangeable photocathode. A copper photocathode, prepared using argon plasma treatment and a 250°C anneal, will provide sufficient quantum efficiency, low mean transverse energy, fast response time and long lifetime.

The diffraction beamline has a magnetic arc which can simultaneously compresses the beam and reduce arrival time jitter, both to the 10 fs level. This is followed by optics to focus the beam into the sample interaction region and provide post sample magnification to the detector. The proposed detector is a 16 MP direct electron detector with single electron sensitivity. Multiple interchangeable sample chambers are proposed for the facility, including a high precision chamber for solid samples, a chamber that can handle gas and liquid phase samples, and a chamber offering ultra-cold temperatures (mK) for quantum materials applications. The final section of the diffraction line will be for ultrafast temporal beam diagnostics.

3.2. Imaging Line

Two separate electron source options are currently being considered for the RUEDI imaging line.

The first is a DC accelerator producing 1-2 MeV electrons with an RF transverse deflecting structure followed by an aperture and a second RF deflector to create the bunches. This arrangement will have low energy spread ($< 3 \times 10^{-5}$), providing good imaging resolution and the capability for stroboscopic measurements with 10 to 200 ps temporal scales. However, 'single shot' measurements might require many pulses and would likely be limited to temporal resolutions above 1 µs.

The second solution uses three RF cavities, an S-band photoinjector, a 4th harmonic lineariser, and a de-chirping/decelerating S-band cavity to achieve 2 MeV energy bunches. The energy spread would likely be 3×10^{-5} or greater and the temporal resolution would be 0.5 to 12 ps. The effect of jitter from the three cavities is a potential issue for this design.

The objective lens is the key element in the imaging system as it needs to provide access for the sample holder, incoming pump laser and probe electron pulses. The solenoidal lens must have very low chromatic aberrations to provide the imaging resolution desired. The imaging system needs to provide magnification in excess of 9,000 and again a single electron sensitive 16 MP direct electron detector will be used.

3.3. Laser Systems

A common oscillator will be used for both the RF source(s) and pump lasers. A wide range of pump laser sources will be provided to both lines to allow a varied and diverse range of experiments to be carried out. A large amount of space has been reserved within the facility for the various laser systems.

4. Environmental Sustainability

RUEDI is the first accelerator designed at Daresbury Laboratory with environmental sustainability taken into account from the outset. A full analysis of the environmental impact has been carried out and is published [1]. In the construction phase the concrete shielding represents the largest cost which is partially mitigated by building RUEDI in and existing radiation-controlled area. During operations the heating and cooling requirements of the rooms and equipment will dominate emissions.

[1] B.J.A.Shepherd et al; 'Sustainability for Particle Accelerators: RUEDI - A Case Study',

Pulsed Laser Deposition Assisted Epitaxial Growth of Cesium Telluride Photocathode for High Brightness Electron Source

Kali Prasanna Mondal[a], Mengjia Gaowei[a], Elena Echeverria[b], Kenneth Evans-Lutterodt[a], Jean Jordan-Sweet[a,c], Thomas Juffmann[d,e], Siddharth Karkare[f], Jared Maxson[b], S.J. van der Molen[g], Chad Pennington[b], Pallavi Saha[a,f], John Smedley[a,h], Guido Stam[g] and Rudolf M. Tromp[c,g]

[a] *Brookhaven National Laboratory, Upton, NY 11973-5000, United States*
[b] *Cornell University Laboratory for Accelerator-Based Sciences and Education, Ithaca, NY 14853, United States*
[c] *IBM T.J. Watson Research Center, Yorktown Heights, NY 10598, United States*
[d] *University of Vienna, Faculty of Physics, VCQ, A-1090 Vienna, Austria*
[e] *University of Vienna, Max Perutz Laboratories, Department of Structural and Computational Biology, A-1030 Vienna, Austria*
[f] *Arizona State University, Tempe, AZ 85287, USA*
[g] *Leiden Institute of Physics, Leiden University, Niels Bohrweg 2, Leiden, The Netherlands*
[h] *SLAC National Accelerator Laboratory, Menlo Park, California 94025, United States Affiliation*

1. Abstract

The epitaxial growth of Cs_2Te photocathodes on various single-crystal substrates has been studied[1]. The growth of an epitaxial layer with a flat surface and high crystallinity is confirmed by reflection high energy electron diffraction (RHEED) for the Cs_2Te thin film. In situ x-ray techniques are used to characterize the film stoichiometry, surface roughness, and crystallinity. Spectral responses are observed, with epitaxial Cs_2Te thin film photocathodes achieving a Quantum Efficiency (QE) of about 17 % of peak value at 270 nm, with a film thickness at 20 nm and a surface roughness of less than 1 nm.

2. Introduction

Photocathodes play an integral role in the development of electron accelerators and photon detectors. Despite having an ultrasmooth photocathode developed by a co-deposition process[2], limitations on the emitted beam brightness persists due to surface and bulk disorder of the polycrystalline photocathode material. Epitaxial growth of photocathodes has the potential to overcome this problem and achieve high-brightness electron beams[3].

In this work, we discuss the findings of Mondal *et al.*[1] where pulsed laser deposition (PLD) is employed to achieve epitaxial growth of Cs_2Te photocathodes on various single-crystal substrates. The study provides a comprehensive analysis of the spectral response of Cs_2Te photocathodes, revealing the influence of substrate choice on the material performance and the electron emission characteristics[1].

3. Experiment

The Cs_2Te deposition process employed PLD, ensuring precise control over the material's stoichiometry and crystalline quality. Comprehensive structural characterization was performed using X-ray diffraction (XRD) and RHEED to assess the crystallinity and surface structure of the films. All experiments were carried out at the 4-ID beamline of the National Synchrotron Light Source II (NSLS-II) at Brookhaven National Laboratory (BNL), leveraging its advanced X-ray capabilities for in-depth material analysis. Further details on the experimental setup, deposition parameters, and characterization techniques can be found in Mondal *et al.*[1].

4. Results and Discussion

Figure 1 shows RHEED images of a 20 nm Cs_2Te film grown on a 4H-SiC substrate, captured at two azimuthal angles spanning a 30° range about the surface normal. The observed streaky pattern indicates smooth surface with small domains, characteristic of high-quality thin films[4]. The azimuthal angular dependence in RHEED patterns, clearly observed in Fig. 1, further confirms epitaxial growth, demonstrating strong in-plane crystallographic alignment with the substrate. This streaky pattern was also observed in RHEED images of Cs_2Te films grown on other single-crystal substrates, highlighting the uniformity of the deposition process. X-ray Reflectivity (XRR) measurements were performed to determine the film thickness and surface roughness. For the 20 nm-thick Cs_2Te films, an ultrasmooth surface with a roughness of less than 1 nm was consistently observed. The smooth surface and crystalline quality minimize grain boundary scattering and reduce mean transverse energy (MTE), making these films ideal for high-brightness electron sources[5]. XRD analyses corroborated these findings, providing additional confirmation of epitaxial coordination and in-plane crystal orientation. X-ray Fluorescence (XRF) measurements, conducted in real-time during growth and after deposition, confirmed the stoichiometric composition of the Cs_2Te films, a key requirement for achieving optimal quantum efficiency (QE). The spectral response of the Cs_2Te photocathodes was measured over the 200 – 400 nm wavelength range. The films exhibited a peak QE of approximately 17 % at 270 nm, achieved with a film thickness of 20 nm. This high QE underscores the superior performance of the epitaxially grown Cs_2Te photocathodes, which are well-suited for high-brightness electron beam applications.

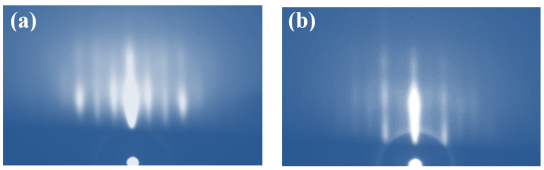

Figure 1. RHEED images of epitaxially grown Cs_2Te on 4H-SiC.

5. Conclusion

In conclusion, the epitaxial growth of Cs_2Te photocathodes on various single-crystal substrates has been successfully demonstrated, achieving ultrasmooth surfaces with roughness below 1 nm. The films exhibit a high peak QE of 17 % at 270 nm, confirming their potential for high-efficiency electron emission. These results highlight the promise of epitaxial growth techniques in advancing the development of high-performance photocathodes for the next-generation accelerators and photon detection systems

6. Outlook and Future Work

Smooth Cs_2Te photocathodes with high QE have been developed. Future efforts will focus on further improving the performance by measuring the emittance of Cs_2Te photocathodes, which will provide valuable insights into their applicability for high-brightness electron beam generation and advanced accelerator technologies.

7. Acknowledgement

The authors would like to acknowledge John Walsh, Rudy Begay and Raul Acevedo-Esteves for technical support of this work. Work is supported by Brookhaven Science Associates, LLC under DE-SC0012704 with the U.S. Department of Energy. This research used resources of beamline 4-ID, ISR, of the NSLS-II, a U.S. Department of Energy (DOE) Office of Science User Facility operated for the DOE Office of Science by BNL under same Contract No. DE-SC0012704.

[1] K.P. Mondal *et al.*; Pulsed laser deposition assisted epitaxial growth of cesium telluride photocathodes for high brightness electron sources; under revision; 2024
[2] M. Gaowei *et al.*; Phys. Rev. Accel. Beams; 2019; 22; 073401
[3] C.T. Parzyck *et al.*; Phys. Rev. Lett.; 2022; 128; 114801
[4] S. Hasegawa; Characterization of Materials; 2012; 97; 925-1938
[5] A. Galdi *et al.* in Proc. IPAC'21, Campinas, Brazil, May 2021, pp. 2979-2982

PhoTEx - Photoemission and Transverse Energy Experiment

Jonas Dube[a,b], **Julius Kühn**[a] **and Thorsten Kamps**[a,b]

[a] *Helmholtz-Zentrum Berlin für Materialien und Energie, Berlin, Germany*
[b] *Humboldt-Universität zu Berlin, Berlin, Germany*

1. Abstract

The **Pho**toemission and **T**ransverse **E**nergy E**x**periment 'PhoTEx' is a novel instrument for the characterization of photocathodes sensitive to visible light. The device was build as a stand-alone drift tube spectrometer. A tunable light source allows the illumination of the cathode in the full visible regime. Simulations showed that the instrument will be able to measure the MTE in the range of 40 meV up to 5 eV with a relative uncertainty of 10 %. PhoTEx is fully assembled and ready to measure the first photocathode.

2. Introduction

The performance of a photocathode used for electron accelerators can be described by three key parameters: the quantum efficiency (QE), the mean transverse energy (MTE) and the lifetime. The mean transverse energy is a figure of merit to produce electron beams with high brightness and is closely related to the transverse emittance $\epsilon_{x,y}$ as shown in Eq. 1. In this case $\sigma_{x,y}$ is the size of the light spot illuminating the photocathode.

$$\epsilon_{x,y} = \sigma_{x,y}\sqrt{\frac{MTE}{mc^2}} \tag{1}$$

At Helmholtz-Zentrum Berlin bi-alkali antimonide photocathodes are developed and researched for several years.[1] They will be used as electron source in the photoinjector of the *Superconducting RF Electron Accelerator Laboratory* (SEALab). Until now there was no device to measure the MTE at HZB.

3. PhoTEx

PhoTEx is designed as a stand-alone system which enables even long time studies without interrupting the growth of new photocathodes. The emitted electrons are accelerated towards an electric conductive grid. The electron beam is widening up behind the grid until it hits an MCP detector. Two pairs of Helmholtz coils are placed around the drift tube to compensate for external magnetic fields e.g. the Earth's magnetic field. A movable pick-up anode can be inserted between the photocathode and the grid to perform QE measurements.

A tunable light source allows the illumination of the photocathode in the full visible regime. The optical power and spot size at the photocathode can be adjusted with a minimum spot size of 130 µm. A reference light path allows continuous monitoring of light power or shape. The optical power of the light reflected by the cathode can be measured to perform a reflectivity measurement.

Table 1. Technical data of PhoTEx.

Measurements:	MTE, QE, lifetime, reflectivity
Acceleration gap g:	10 mm
Drift distance d:	300.9 mm
Bias voltage U:	< 6.5 kV
E-field:	< 0.65 MV/m
Sample holder:	Omicron flag style
Detector:	MCP with gain 10^4 + P43 phosphor screen
Light source:	Zolix tunable light source TLS2-X75A-G
Spectral regime:	(400-700) nm
Bandwidth:	5 nm
Illumination angle:	38.7°
Spot size:	> 130 µm

[1] S. Mistry et al.; Proc. IPAC'23 pp. 4291-4293, May 2023

4. Simulations

In the idealized case the electrons are accelerated in a perfect homogeneous electric field with voltage U and length g, before they drift in a field-free drift region of length d. In this case the MTE can be calculated by the simple analytical formula in Eq. 2 from the mean radius of the electron distribution at the detector r_{mean}.[2]

$$MTE = \frac{r_{mean}^2}{(2g+d)^2}Ue \tag{2}$$

To test the performance of the device, the measurement procedure was simulated. A 3D simulation of the electric field inside the vacuum chamber was performed using CST Studio. Afterwards, the electron path through the simulated fields was simulated by numerical tracking with ASTRA. As expected the electric field is not perfectly homogeneous in reality, resulting in a deviation of about 12 % between the input and the simulated value. This leads to a total uncertainty of about 20 %, already including the Davisson-Calbick effect, detector resolution, fit and measurement uncertainties.[3] A numerical method was developed to calculate the MTE by tracking through the simulated fields instead of using the analytical formula. With this method the total uncertainty can be reduced to 10 %. This uncertainty can be achieved as long as the electron beam has an appropriate spot size at the detector and is fully independent of the specific MTE or bias voltage. Therefore, the measurement range of PhoTEx is solely limited by the acceleration voltage. With our maximum bias of 6.5 kV it is possible to measure MTE's of more then 5 eV. The lower limit depends on how low the voltage can be reduced before external fields become relevant. With a voltage of 1 kV an MTE down to 40 meV would be possible.

5. Status and Outlook

PhoTEx is currently fully assembled and under vacuum. A base pressure of $< 1 \cdot 10^{-10}$ mbar was achieved. The commissioning is in progress and the system is ready for the first photocathode which will follow within the next month. PhoTEx will increase the data output and efficiency of the photocathode laboratory at HZB. As far as is known, PhoTEx is the first instrument which is able to measure the full set of physical parameters of photocathodes relevant for particle accelerators. It is therefore a powerful tool for the generation of high brightness beams and the investigation of the photoemission process.

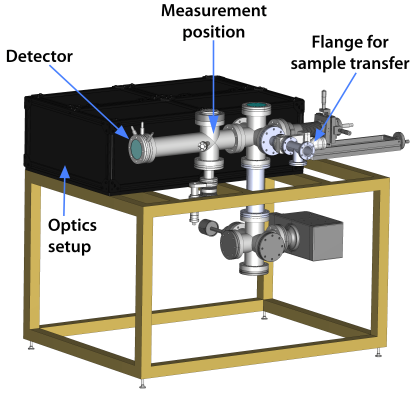

Figure 1. 3D model of PhoTEx.

[2] J. Feng et al.; Rev. Sci. Instrum. **86**, 015103 (2015)
[3] L. Yu et al.; Rev. Sci. Instrum. **92**, 013302 (2021)

Atomically smooth films of CsSb: an alternative visible light photocathode

Alice Galdi[a] and C.T. Parzyck,C.A. Pennington, W.J.I. DeBenedetti, J. Balajka, E.M. Echeverria, H. Paik, L. Moreschini, B.D. Faeth, C. Hu, J.K. Nangoi, V. Anil, T.A. Arias, M.A. Hines, D.G. Schlom, K.M. Shen, J.M. Maxson[b]

[a] *Universitá degli Studi di Salerno, Italy*
[b] *Cornell University, NY, USA*

1. Abstract

Cs_3Sb and related alkali antimonide compounds are high efficiency semiconductor photocathodes that can be operated with visible light and possess quantum efficiency of the order of 1-10% at green light wavelength. Use of these photocathodes in modern linear accelerators is desirable thanks to their potential to generate high brightness electron beams. However, the ultimate brightness of a photocathode is limited by surface disorder of the usually polycrystalline and inhomogeneous films. We used state-of-the-art molecular beam epitaxy to achieve epitaxy of the Cs_3Sb phase for the first time, thus realizing ordered, homogeneous surfaces. Furthermore, using in-situ electron diffraction as a structural probe during growth, instead of quantum efficiency, we were able to stabilize atomically flat films with composition Cs:Sb 1:1, a phase characterized by higher photoemission threshold than Cs_3Sb, having 1% quantum efficiency at 405 nm and higher resistance to oxygen poisoning.

2. Introduction

In recent years, accelerator scientists have identified high efficiency semiconductor photocathodes as the choice of photoemission sources for new generation light sources and other high-performance electron accelerators. In particular, the minimization of emittance at the cathode is considered paramount to optimize these machines.[1] For a given material, the lowest achievable emittance is proportional to the average transverse momentum spread of the photoelectrons. The new generation of linear accelerators is pushing the required beam quality to the point that even the contribution of the nanoscale roughness of the photocathode surface matters.[2] This led to many studies devoted to synthesize high efficiency alkali antimonides in form of ordered crystalline films as opposed to the usual disordered photoemissive coating. Recently, epitaxy of Cs_3Sb was achieved on single-crystal substrates, allowing to synthesize ultrathin (4-10 nm thick) samples with high quantum efficiency (QE), especially in the vicinity of the photoemission threshold. This achievement was made possible by the use of state-of-the-art molecular beam epitaxy (MBE) and by the use of reflection high energy electron diffraction (RHEED) to monitor the structure of the sample's surface during growth.[3]

By monitoring the structure instead of quantum efficiency during MBE growth, we had the opportunity to explore a different phase of Cs-Sb, CsSb, characterised by atomically flat surfaces when grown on suitable substrates, despite not presenting epitaxy.

3. Results and Discussion

Atomically smooth films with CsSb composition can be obtained by codeposition of Cs and Sb at temperature higher than the one required for the stabilisation of the Cs_3Sb phase. Typical deposition conditions are Cs flux of about $1.6 \times 10^{+13}$ atoms/cm^2/s, Sb flux of about 2.5×10^{12} atoms/cm^2/s and a substrate temperature of 160-200 °C, although the optimal growth temperature depends on the Cs partial pressure.

In appropriate conditions, closely spaced streaks appear in the RHEED pattern within the first 10-30 min of growth. An example is shown in Figure 1, where the Cs_3Sb RHEED pattern is compared to the CsSb one. Both samples are grown on 3C-SiC (100) substrate. An important difference between the two samples can be observed when rotating the sample around its surface normal: while the pattern of Cs_3Sb changes, by showing the in-plane alignment of the film with the substrate, the CsSb pattern remains the same, demonstrating no specific in-plane arrangement of the crystalline structure of the film. The 2D character of the RHEED pattern is the signature of an atomically flat surface. Scanning tunnel microscopy measurements performed on some CsSb samples reveal flat terraces with a step height of about 0.7 nm, and the presence of ordered atom rows that change direction at the step edges.

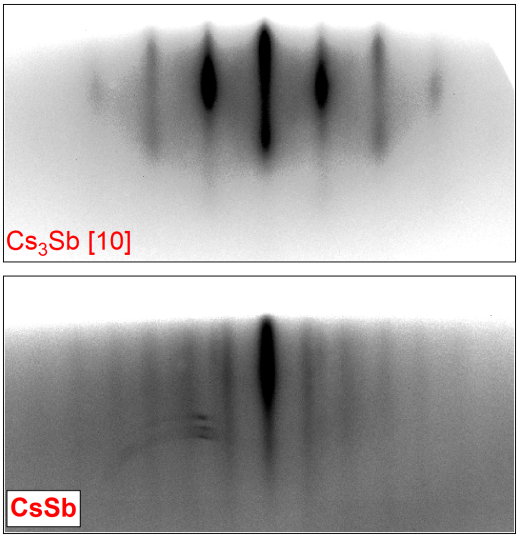

Figure 1. Comparison of RHEED patterns of Cs_3Sb // along the [10] azimuth (top) and of CsSb (bottom).

The spectral response of CsSb atomically flat films reveals that the photoemission threshold for this compound is about 2.2 eV (566 nm), with a quantum efficiency of about 1% at 400 nm. The quantum efficiency at 520 nm is of the order of 10^{-4}. In order to characterize the chemical resistance of CsSb against poisoning, oxidation experiments were performed by exposing the photocathode to a controlled dose of oxygen gas at a pressure between $5 \times 10^{-9} - 5 \times 10^{-8}$ Torr, and by measuring the photocurrent decay at 405 nm. The loss of quantum efficiency was compared to the behavior of a Cs_3Sb photocathode at 532 nm. The results show that to obtain the same proportional decrease of quantum efficiency, CsSb requires an oxygen dose about 10 times higher than Cs_3Sb.[4]

4. Outlook and Future Work

The results, which are discussed in details in ref.4, demonstrate that it is possible, by using state-of-the-art synthesis and analysis techniques, to experimentally explore the phase diagram of various compounds and discover phases with interesting physical properties for application as high performance photocathodes.

[1] J. Maxson *et al.*; Appl Phys Lett 2015 **106** 234102
[2] J. Lewellen *et al.*; JACoW NAPAC2022, TUYD3
[3] C. T. Parzyck, A. Galdi *et al.*; Phys Rev Lett 2022 **128** 114801
[4] C.T. Parzyck *et al.*; APL Mater 2023; **11**: 101125

Development of Multi-Alkali Antimonide Photocathodes for High-Brightness Photoinjectors

S.K. Mohanty[a,b], M. Krasilnikov[a], A. Oppelt[a], F. Stephan[a], D. Sertore[b] and L. Monaco[b]

[a] *DESY, Zeuthen, Germany*
[b] *Istituto Nazionale di Fisica Nucleare - LASA, Segrate, Italy*

1. Abstract

Multi-alkali antimonide photocathodes, particularly potassium-cesium-antimonide, are highly suitable for high-repetition-rate FEL applications due to their photoemissive properties, including low thermal emittance and high sensitivity in the green wavelength. To evaluate their performance in high-gradient RF guns, DESY collaborated with INFN LASA to develop multi-alkali photocathode materials. In June 2024, as part of the second batch, three KCsSb cathodes and one NaKSb(Cs) cathode were produced, successfully transferred, and tested in the PITZ high-gradient RF gun. This contribution summarizes the growth procedures and preliminary experimental results obtained from these second-generation multi-alkali antimonide cathodes.

2. Fabrication Recipes

A total of four photocathodes were produced through sequential deposition on INFN Mo plugs: Cathode 99.1 (thin multi-layer KCsSb), Cathode 124.1 (thin KCsSb with controlled K thickness), Cathode 128.1 (thick KCsSb with controlled K thickness), and Cathode 131.1 (NaKSb(Cs)). A microbalance issue during Na deposition on Cathode 131.1 resulted in low QE; therefore, this cathode is excluded from further data analysis. The detailed fabrication procedures are described below.

2.1. Cathode 99.1

To prevent Sb crystallization, 3 nm of Sb was initially deposited on the Mo substrate, as crystallization typically begins around 4–6 nm, according to previous studies [1]. Furthermore, AFM studies indicate that when alkali metals diffuse into crystalline Sb, they can induce stress and structural changes, increasing roughness and forming nano-pillar structures [2]. Therefore, we deposited 3 nm of Sb at a rate of 1 nm/min at ~ 100°C to avoid crystallization. Thereafter, K was deposited at 0.6 nm/min at 120°C until the maximum photocurrent was reached, followed by Cs at 0.8 nm/min at 110°C until photocurrent saturation. A second KCsSb layer was then deposited on top of the first layer using a similar process.

2.2. Cathode 124.1

For cathode 124.1, we deposited 5 nm of Sb at 1 nm/min, followed by K until the thickness reached approximately 36 nm, based on the transition point where the KSb compound typically transforms from amorphous to crystalline [1]. K deposition was stopped at this point to preserve the cubic form of the KSb compound. Cs was then deposited until the photocurrent approached saturation. The substrate temperature and deposition rates for Sb, K, and Cs were the same as those used for cathode 99.1.

2.3. Cathode 128.1

For cathode 128.1, K was deposited up to 54 nm (up to the transition point) following the same procedure as for cathode 124.1, with the difference in total thickness due to the initial 10 nm Sb layer. Cs was deposited until photocurrent saturation. The substrate temperature and deposition rates for Sb, K, and Cs were the same as those used for cathode 124.1.

3. Results

Previous XRD studies show that K thickness affects the crystal structure: cubic K_3Sb forms near the transition point, while hexagonal

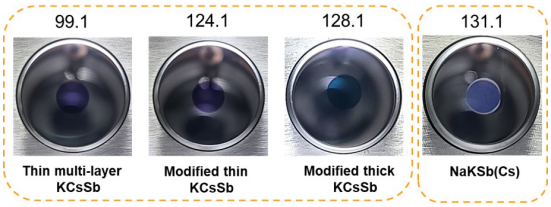

Figure 1. Photographs of the second batch of alkali antimonide cathodes.

K_3Sb forms at a later stage during K deposition. Cs reacts effectively with cubic K_3Sb, forming predominantly cubic K_2CsSb [1,3]. For cathodes 124.1 (modified thin) and 128.1 (modified thick), K deposition was intentionally stopped near the transition point to achieve a cubic KSb compound, ultimately resulting in a cubic KCsSb compound. Spectral reflectivity measurements (Fig. 2) conducted after the formation of the KSb compound showed similar behavior for both cathodes, with peaks at 2.70 eV (C'), a local minimum at 3.06 eV, and a peak (F') around 3.9 eV for cathodes 124.1 and 128.1. When compared with the DFT-calculated spectral reflectivity of K_3Sb (cubic), the corresponding C' and F' peaks appear at 2.67 eV and 3.89 eV, respectively [1]. This similarity in peak positions suggests that the KSb compounds in both cathodes (cathodes 124.1 & 128.1) exhibit a cubic crystal orientation. A similar comparison of the spectral reflectivity peaks of the KCsSb compounds from cathodes 124.1 and 128.1, between experimental data and DFT calculations, was conducted and revealed good agreement in peak positions, suggesting that the grown compound is predominantly cubic.

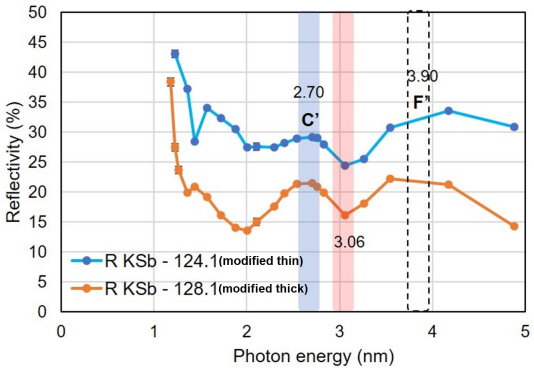

Figure 2. Spectral Reflectivity of KSb for Cathodes 124.1 and 128.1

After production, the cathodes were successfully transported and tested at the PITZ RF gun, showing uniform QE maps and no significant vacuum events observed during operation. However, the lifetimes of these three cathodes were observed to be about 3 days during operation in the gun.

4. Outlook and Future Work

This report presents a summary of the growth procedure and the preliminary results of the second batch of KCsSb cathodes. Further data analysis is in progress. Comprehensive results will be shared in future publications.

[1] S.K. Mohanty, Dissertation, University of Hamburg (2024)
[2] S. Schubert *et al.*, APL Materials, 1(3), 032119 (2013)
[3] S. Schubert *et al.*, Proc. IPAC 2014, MOPRI018, 624 - 626 (2014)

High QE Photocathode Preparations and Tests at SHINE

Xudong Li[a], Zenggong Jiang[a], Hao Meng[a], Qiang Gu[a], Houjun Qian[b], Guan Shu[b], Zipeng Liu[b], Qin Zhou[b] and Chaochao Xing[b]

[a] *Shanghai Advanced Research Institute, Chinese Academy of Sciences*
[b] *Zhangjiang Laboratory*

1. Abstract

The Shanghai Advanced Research Institute (SARI) has completed the design, assembly, and debugging of the photocathode preparation system and photocathode load lock system. The typical process of a stable and repeatable high-quality Cs_2Te photocathode preparation is to apply Te intermittent, Cs continuous deposition has been developed with SHINE photocathode preparation system. The quantum efficiency (QE) of Cs_2Te photocathode is greater than 5 % under 265 nm light irradiation. The Cs_2Te photocathode prepared by Te intermittent and Cs continuous deposition method for the first time is used in SHINE VHF electron gun operation.

2. Introduction

As far as I am concerned, the characteristics of the ideal photocathode are: high quantum efficiency(QE, ideally ~ 100 %) at long wavelength light, reasonable lifetime(> 1 year) in a practical vacuum (10^{-6} Pa), short response time (~ ps), low emittance (low mean transverse energy), dark current can be ignored. Although there are several typical high QE semiconductor photocathodes could be chosen by SHINE (Shanghai HIgh repetitioN rate XFEL and Extreme light facility). The Cs_2Te photocathode can be selected for SHINE electron gun when these various factors are considered.

3. Photocathode Systems

The photocathode systems integrate the following functions: loading, cleaning, preparation, and transfer. The photocathode systems are composed of photocathode preparation system, photocathode suitcase, photocathode load lock system. The photocathode suitcase can be used to transport the Cs_2Te photocathode between the photocathode preparation system and photocathode load lock system.

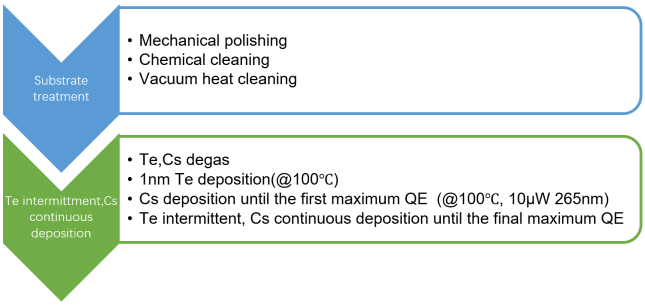

Figure 1. The typical Cs_2Te photocathode preparation process with Te intermittent and Cs continuous deposition.

4. Photocathode Preparation

Te intermittent and Cs continuous deposition[1] of the high QE Cs_2Te photocathode is developed by drawing on the GaAs photocathode Yo-Yo activation method of Cs and O. The typical Cs_2Te photocathode preparation process with Te intermittent and Cs continuous deposition is shown in Figure 1. The optimal Te thickness for high QE Cs_2Te photocathode is about 6 – 7 nm. The change of QE, reflectivity and thickness with time in the process of Cs_2Te photocathode preparation is shown in Figure 2.

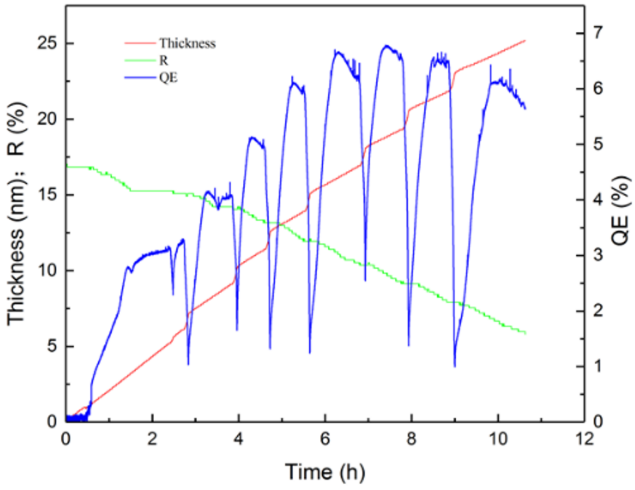

Figure 2. The change of QE, reflectivity and thickness with time in the process of Cs_2Te photocathode preparation.

5. Photocathode Tests

The prepared Cs_2Te photocathode can be transported from the photocathode preparation device to the SHINE VHF electron gun by the photocathode suitcase. The distance between the photocathode preparation device and VHF electron gun is about 1 km. The Cs_2Te photocathode must be in UHV to maintain its performance. The Cs_2Te photocathode prepared by Te intermittent and Cs continuous deposition method can operate for a long lifetime in the SHINE VHF electron gun at 50 pC and 100 pC, and the repetition rate is 1 MHz as shown in Figure 3.

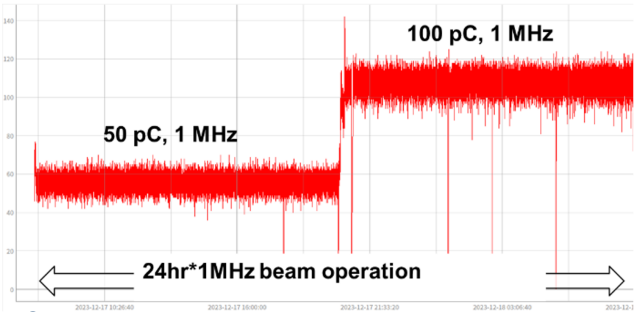

Figure 3. The Cs_2Te photocathode operation at 50 pC and 100 pC.

6. Outlook and Future Work

Provide Cs_2Te photocathodes required for SHINE VHF electron gun[2] and provide photocathodes for more electron guns. Identify which parameters impact the operation lifetime of Cs_2Te photocathode in SHINE VHF electron gun. It is necessary to optimize the photocathode preparation process based on the actual requirements of SHINE VHF electron gun, study on the photocathode properties during the preparation process to prepare photocathodes with better performance and prepare many various types of high QE photocathodes.

[1] X.D. Li *et al.*; *Cs-Te photocathode preparation with Te intermittent and Cs continuous deposition based on improved preparation success rate and quantum efficiency*; Acta Phys. Sin. 71(17) 178501 (2022)

[2] L.M. Zheng *et al.*; *Design, fabrication, and beam commissioning of a 216.667 MHz continuous-wave photocathode very-high-frequency electron gun*; Phys. Rev. Accel. Beams **26**, 103402 (2023)

Machine Learning-Assisted Design of Cs-Based Photocathode Materials from First Principles

Holger-Dietrich Saßnick[a] **and Caterina Cocchi**[a]

[a]*Carl von Ossietzky Universität Oldenburg, Physics Department, 26129 Oldenburg*

1. Abstract

Ab initio methods such as density functional theory (DFT) are successfully used to complement experimental research on photocathode materials. However, these methods also require structural information as an input, limiting their application to experimentally known crystal structures. To overcome this drawback, a novel approach combining high-throughput calculations and machine-learning models is proposed as a viable way to derive stable crystals. Its application to Cs-Te binary compounds demonstrates its potential.

2. Motivation & Methodology

Crystal structure prediction (CSP) methods aim to determine the ground-state crystal structure for a given material. Their high computational demand is common to all these methods, prohibiting their widespread application. Machine learning models have proven to be a promising route to derive structure-property relationships efficiently. Here, we combine *high-throughput* DFT calculations with machine learning (ML) to predict stable crystals. We apply it to Cs-Te binary compounds which are used as photocathodes in several particle-accelerator facilities around the globe.

All DFT calculations carried out in this work are performed with the package `CP2K`[1] using double-ζ basis sets and Goedecker-Teter-Hutter pseudopotentials[2] to describe the core electrons. The plane wave (relative) cutoff is set to 450 Ha (75 Ha), and PBE [3] is used to approximate the exchange-correlation potential. DFT calculations and ML models are embedded in a high-throughput workflow developed within the Python library `aim²dat`[4] interfaced with the `AiiDA` infrastructure[5].

Two different types of ML models are used. The models based on the *Coord.* descriptor (implemented in `aim²dat`) encode the coordination environment of the atom sites and use the extremely randomized trees (*ET*) or kernel ridge regression (*KRR*) algorithms (relying on the `scikit-learn` infrastructure) to predict the stability. The *M3GNet* models[6] are graph neural networks that have been pre-trained on more than 60,000 crystals. While the *M3GNet TF* model is transfer-trained, the *M3GNet base* model merely relies on the pre-training.

3. High-Throughput Dataset

As a first step, a large pool of randomly generated crystals, covering Cs concentrations $\in [0, 1]$ as well as different crystal symmetries and space group is allocated using the `PyXtaL`[7] Python package. The forces at each atomic site and the pressure are optimized via *high-throughput* DFT calculations. With 34.2 % of the input crystals failing due to numerical issues, the final dataset consists of 1073 relaxed crystals. The stability of each crystal (ΔE_{Hull}) is evaluated based on the distance of their formation energy to the convex hull. As such, zero-point energy and thermal contributions are neglected. To train the ML models, the dataset is split up in a stratified manner, resulting in multiple training sets ranging from 100 to 600 crystals and test sets with the remaining 473 structures.

[1] T. D. Kühne *et al.*, *J. Chem. Phys.*, vol. 152, no. 19, p. 194103, May 2020
[2] S. Goedecker, M. Teter, and J. Hutter, *Phys. Rev. B*, vol. 54, no. 3, pp. 1703–1710, Jul. 1996
[3] J. P. Perdew, K. Burke, and M. Ernzerhof, *Phys. Rev. Lett.*, vol. 77, no. 18, pp. 3865–3868, Oct. 1996
[4] aim2dat github repository, https://github.com/ aim2dat/aim2dat, accessed: 2024-11-18.
[5] S. P. Huber *et al.*, *Sci. Data*, vol. 7, no. 1, p. 300, Sep. 2020
[6] C. Chen and S. P. Ong, *Nat Comput Sci*, vol. 2, no. 11, pp. 718–728, Nov. 2022
[7] S. Fredericks *et al.*, *Comput. Phys. Commun.*, vol. 261, p. 107810, Apr. 2021

4. Performance of the ML Models

The mean absolute error (MAE) is used as a metric to compare the accuracy of the different ML models, see Fig. 1. Since the *Coord. ET* and the *Coord. KRR* models use the same descriptor; both models exhibit similar errors of about 0.05 eV/atom for the largest training sets. The transfer-trained *M3GNet* model outperforms the others, producing errors below 0.04 eV/atom. On the other hand, the base variant of the *M3GNet* delivers the worst performance. This behavior is not unexpected considering that this model was not on this dataset.

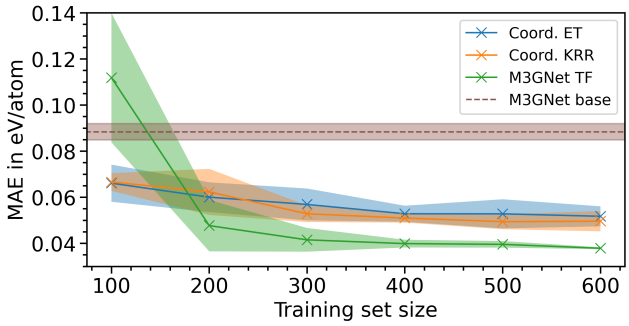

Figure 1. Average mean absolute error (MAE) over the three random splits and its standard deviation (shaded area).

5. Pre-Selection of Stable Crystals

A second structure pool, mirroring the first and containing 15,000 crystals, is generated in the last step. To expedite the process, ML models are employed to pre-screen candidates instead of brute-force DFT calculations. To enhance the chances of identifying stable structures, a grid search is applied to each crystal varying the cell vector lengths and angles while keeping the symmetry constrained. The most stable crystal variant is finally selected. Based on the predictions, 100 crystals are chosen for each model and validated via DFT calculations, see Tab. 1. In contrast to the test sets displayed in Fig. 1, the *Coord.* models show the best performance and result in the largest fraction of stable crystals.

Table 1. Mean of the calculated stability (ΔE_{Hull}) and MAE of the predicted stability in eV/atom; success rate (S.R.) of the *high-throughput* workflow and fractions of stable phases with Te/mixed/Cs content. Results delivered by the best-performing models are highlighted in bold.

	ΔE_{hull}	**MAE**	**S.R.** (%)	**Stable crystals** (%)
Initial pool	0.212	–	65.8	0.0/2.1/1.3
Coord. ET	0.178	**0.081**	**90.0**	**0.0/6.0/5.0**
Coord. KRR	0.164	0.101	80.0	0.0/5.0/5.0
M3GNet TF	0.195	0.110	**90.0**	1.0/5.0/1.0
M3GNet base	0.193	0.156	77.0	0.0/4.0/3.0

6. Conclusions & Future Work

In conclusion, our method provides a promising pathway to explore the configurational space and identify stable crystal structures for experimentally challenging materials, including ternary systems like multi-alkali antimonides.

OptaDOS Photoemission - The Good, The Bad, The Interesting

Felix Mildner[a,c] **and Nicholas M. Harrison**[b]

[a]*Imperial College London, Dept. Materials*
[b]*Imperial College London, Dept. Chemistry*
[c]*CDT Advanced Characterisation of Materials*

1. Abstract

Modelling the photoemission response of materials using first-principle calculations is a useful tool to aid in the validation of experimental results and the development of new materials and hetero-systems for future applications in photocathodes.

The OptaDOS Code[1] is a widely used, open source tool to calculate densities of states and optical properties from first principle calculations. This work is part of extending OptaDOS capabilities to calculate photoemission properties of slab models. Comparing the calculated mean transverse energy (MTE) curve for a Cu(100) slab geometry to the extended Dowell-Schmerge (DS) Model[2] shows the contrast between the non monotonic calculated MTE curve and the smooth increase of the extended DS-Model. Efforts to improve the calculated MTE response curve and allow calculation of the response for supercell geometries accurately are ongoing.

A brief description for different parts of the implemented model and a comparison to other models is given.

2. The OptaDOS Photoemission Model

The OptaDOS code in its current state is written to work best with the CASTEP *ab-initio* modelling package[3] but the relevant data can be taken from any electronic structure code and formatted into the openly accessible data scheme. An exemplary workflow using CASTEP and OptaDOS is given in Figure 1. Some data is calculated using the relevant electronic structure code and the user can supply a number of parameters controlling the calculation, such as the light polarisation, temperature, emission model and more.

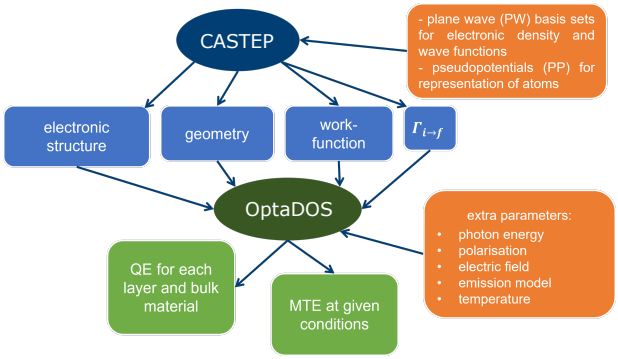

Figure 1. General workflow and parameters used to calculate the photoemission response of a material using CASTEP and OptaDOS. $\Gamma_{i\to f}$ is the transition probability between two bands of the electronic structure.

The electronic excitations and emission are calculated explicitly and k-point resolved, rather than taking the density of states (DOS) averaged across the reciprocal cell. The quantum efficiency (QE) and transverse energy contributions from slab layers, atoms, bands, and K-points are calculated using either a 3-Step or 1-Step model.

The excitation step probability is calculated using a Fermi's Golden Rule type formalism into either a Bloch state for the 3-Step model or a dampened plane wave for the 1-Step model. The depth based escape probability is calculated using a mean free path model with a spectroscopic constant and the explicit slab layers are extended using a bulk region approximation of repeated bulk-like layers. The MTE is calculated using a weighted sum of all contributions and their associated transverse energy.

3. Comparison to other Models and Experiments

To compare an MTE curve generated by OptaDOS photoemission against the extended DS model and experimental data[4] a Cu(100) 16 layer slab with a Monkhorst-Pack (MP) grid of 512x512x1 and a vacuum gap of 15Å modelled in CASTEP. The OptaDOS Photoemission model was then used to calculate the MTE response curve. The graph comparing the three different curves is given in Figure 2.

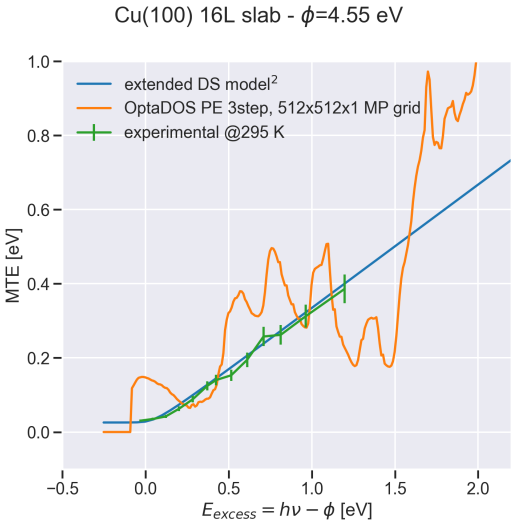

Figure 2. Comparison of MTE response curves of Cu(100) surface from experimental data, the extended DS model[2] and calculated using OptaDOS.

The non-monotonic features of the calculated MTE response curve are very evident, whereas both the experimental data and extended DS model[2] show a smooth increase. The overall trend, however, is comparable for the given energy range. It is highly unlikely that the non-monotonic response is caused by undersampling the reciprocal space given the very tight sampling grid used. It is more likely this stems from the weighted sum approach to calculate the MTE, whereas the extended DS model uses a smooth function with respect to E_{excess}.

4. Outlook and Future Work

The Photoemission module is currently being prepared for integration into the official release of OptaDOS. At the moment the k-point resolved calculation of emissions is incompatible with supercell geometries and their so called "folded" band structure. Representing multi-material structures and defective surface structures requires the use of supercells. Thus the ability to deal with such systems is a major goal for the near future. Further efforts to improve the calculated MTE response curves in comparison to experimental data and other emission models are ongoing.

[1] A.J. Morris, R.J. Nicholls, C.J. Pickard, and J.R. Yates, Computer Physics Communications 4 February 2014; **185** (5): 1477-1485.
[2] T. Vecchione, D.H. Dowell, W. Wan, J. Feng, and H.A. Padmore, Proceedings of FEL, New York, 2013
[3] S.J. Clark et al., Zeitschrift fuer Kristallographie 1 May 2005,**220**(5-6): 567-570
[4] C. Benjamin, EWPAA 2022 Contributed Talk 21 September 2022, Milan

An Overview of MTE Measurement Techniques and Photocathode R&D at Daresbury Laboratory

Lee Jones[a,b]

[a] *STFC Daresbury Laboratory, Sci-Tech Daresbury, Warrington, Cheshire, WA4 4AD, United Kingdom*
[b] *The Cockcroft Institute, Sci-Tech Daresbury, Warrington, Cheshire, WA4 4AD, United Kingdom*

1. Abstract

The ability to characterize the performance of photoemissive materials for use as photocathode electron sources is a crucial aspect of R&D for electron accelerators. The important characteristics include the mean transverse and longitudinal energy spreads (MTE & MLE), spectral response and quantum efficiency (QE). This presentation reviews selected photocathode characterization systems developed over the last 3 decades, and offers a brief update on photocathode R&D activities at the Daresbury Laboratory.

2. 2D Energy Measurement Systems

An ideal energy analyzer would simultaneously measure transverse and longitudinal energy spreads. Such a system was constructed at the Max Planck Institute in Heidelberg by Pastuszka[1] and Orlov[2] around 2000 to support development of an ultra–cold electron source based on GaAs. This inspired work by Karkare[3] *et al.* some 15 years later to develop their 2D analyser at Cornell University shown in Fig. 1, modifying and refining the MPI design. Both systems exploited the combination of magnetic fields to discriminate transverse energy by controlling the radius of gyration of each electron around its guiding centre, and a repulsive electric field applied to an iris (pinhole) to discriminate longitudinal energy. Any electrons passing through the iris and reaching the detector were effectively tagged by this combination of magnetic and electric field, so the reconstruction of the transverse and longitudinal energy distributions was possible.

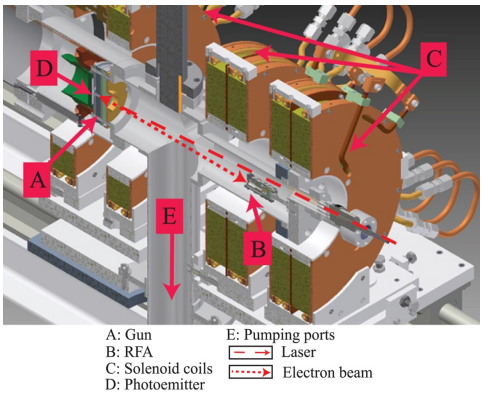

Figure 1. Concept of the Cornell University 2D energy analyser.

3. The 'Momentatron' Measurement System

The 'Momentatron' concept shown in Fig. 2 was developed at LBNL. Its design principle is common within the photocathode research community for photoelectron transverse energy distribution measurement. The concept described by Feng[4] involves the emission of photoelectrons which are first accelerated over a short distance to high energy (typically 10 keV) then allowed to propagate over a known distance before being imaged on a screen. Analysis of the image with knowledge of the flight time and drift distance yields the transverse energy distribution. However imaging solutions such as this suffer a reduction in resolving power as the cathode MTE falls.

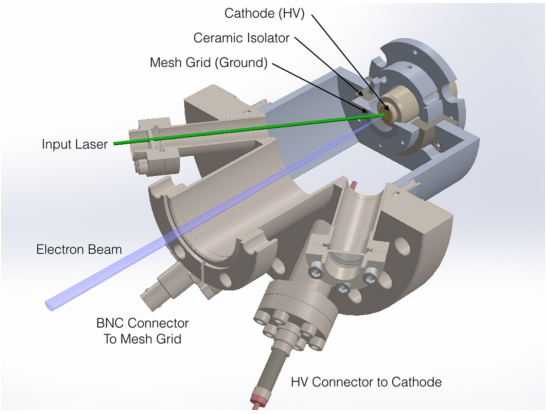

Figure 2. Concept of the LBNL 'Momentatron' MTE measurement system.

4. The Transverse Energy Spread Spectrometer (TESS)

The TESS system is similar to the Momentatron, but involves only low energy electron transport (typically 50 – 80 eV), and is described in detail by Jones[5]. TESS includes a broadband lightsource with sufficient power to measure MTE and QE at any wavelength for all photocathode types, and to study photocathode performance and lifetime under controlled degradation through gas exposure.

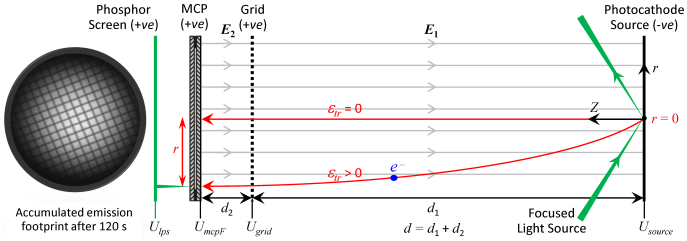

Figure 3. Concept of the TESS MTE measurement system.

5. Photocathode R&D Activities at Daresbury Laboratory

Our photocathode R&D focusses on supporting the CLARA[6] accelerator, and on the development of a high repetition rate RF gun to drive a future UK XFEL. This is synergetic with photoinjector R&D at DESY. We are working through an extensive programme of work to characterise the performance of copper subjected to different preparation techniques. Initial results have shown QE around 3E-4 at 266 nm for Cu cleaned with BPS172 then annealed in vacuum to 250 °C.

We have progressed our work to investigate the practicality of reducing work function and extending the spectral response of copper through caesium ion implantation. Data recently obtained using the MEIS[7] facility demonstrate sub–surface implantation for Cs ion source energies of 2, 3 and 5 keV. We plan to repeat this implantation process with samples in TESS, then measure the QE, spectral response and assess the robustness of the Cs-implanted-Cu system.

We are investigating Rb_2Te as a practical and robust alternative to Cs_2Te. Initial work[8] implies a QE around 3.5 % at 266 nm with XPS data demonstrating the formation of Rb_2Te, but with an excess of Te.

[1] Pastuszka *et al.*; J. Appl. Phys. 88 **(11)**, 6788 - 6800 (2000)
[2] Orlov *et al.*; Appl. Phys. Lett. 78 **(18)**, 2721 - 2723 (2001)
[3] Karkare *et al.*; Rev. of Sci. Instrum. **86**, 033301 (2015)
[4] Feng. *et al.*; Rev. of Sci. Instrum. **86**, 015103 (2015)
[5] Jones *et al.*; Rev. of Sci. Instrum. **93**, 113314 (2022)
[6] Angal-Kalinin *et al.*; Phys. Rev. STAB **23**, 044801 (2020)
[7] Medium Energy Ion Scattering – Barlow *et al.*; Proc. IPAC '12, THPPR075, 4151 - 4153
[8] Benjamin *et al.*; Proc. IPAC '24, WEPC71, 2134 - 2136

Photocathode characterization using a UV-tunable ultrashort pulse radiation source

W. Andreas Schroeder, Ir-Jene Shan and Louis A. Angeloni

Department of Physics, University of Illinois – Chicago

1. Abstract

The design criteria and performance of the tunable-UV photocathode characterization system at the University of Illinois – Chicago are outlined. Low-power UV laser cleaning of single-crystal metal photocathodes is shown to yield work functions in agreement with density functional theory (DFT) calculations.

2. Introduction

Accurate experimental spectral characterization of the electron emission properties of solid-state materials is a key component in the search for new high brightness photocathodes; an improved understanding of the experimental data through theoretical photoemission models allowing for more refined and targeted searches of the vast catalog of known materials[1]. The photocathode characterization system at the University of Illinois Chicago (UIC) with its large 3.0-5.3 eV near-UV spectral coverage is just one example of the type of experimental set-up required to measure the spectral dependence of both the quantum efficiency (QE) and mean transverse energy (MTE) of photoemitted electrons.

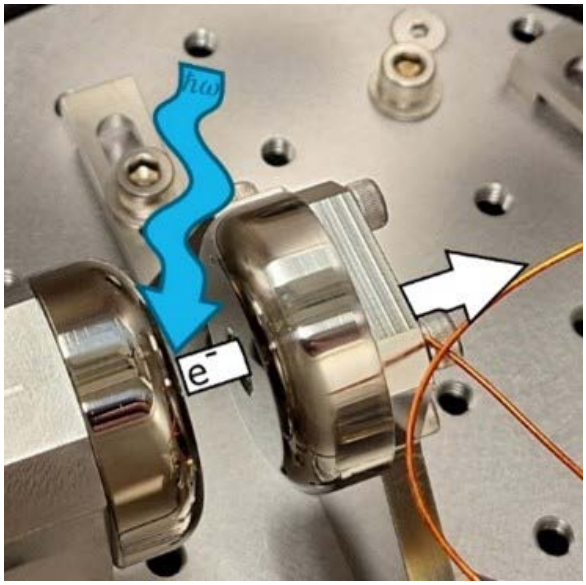

Figure 1. The 10-20 kV DC photoelectron gun

3. Design Criteria

The UIC photocathode characterization system addresses several design criteria: (i) a front-end, high repetition rate (10-100 MHz), sub-picosecond laser to both eliminate intra-pulse space charge effects and facilitate the use of nonlinear optical techniques for wide spectral tunability; (ii) a 'simple' 10-20 kV DC gun (Figure 1) followed by a ~40 cm drift region to allow straightforward electron trajectory simulations for MTE calibration; (iii) Fourier spatial filtering of 60° incident p-polarized UV radiation to minimize laser beam pointing fluctuations, allow the use of 'top-hat' and near Gaussian spatial beam profiles, and reduce photocathode reflection losses; and (iv) a micro-channel plate (MCP) detector with a P43 phosphor screen matched to a low noise CMOS digital camera to provide for high electron detection fidelity. The resulting system is capable of measuring MTE values well below 5 meV and QE values down to $\sim 10^{-10}$.

4. Work Function Determination

The photocathode characterization system is calibrated using a Rh(110) photocathode for which the measured spectral dependences of the QE and MTE are known to be consistent with a band-based photoemission simulation[2]. An integral aspect of this calibration (and other measurements) is the accurate determination of the photocathode's work function ϕ, using the theoretical spectral dependence of the QE, as it sets the excess photoemission energy for the MTE. This means that all spectral characterization measurements are generally performed after exposing the photocathode surface to $\sim 1 W/cm^2$ of 257 nm UV radiation for 20-30 minutes. Monitoring of both the QE and MTE as a function of UV exposure time during this 'laser cleaning' process indicates that the dominant effect is a reduction in the surface work function. For single-crystal metal photocathodes, the UV laser cleaning typically reduces the work function by 0.2-0.5 eV, resulting in values that are in better agreement with preliminary 'perfect crystal' thin-slab calculations based on DFT, as shown in Table 1.

Table 1. Work functions of selected metal photocathodes

Photocathode	$\phi_{expt.}$ (±0.1 eV)	ϕ_{DFT} (±0.1 eV)
Ag(001)	3.94	4.25
Mo(001)	3.89	4.3
Nb(001)	3.94	3.52
Rh(110)	4.13	4.37
Ta(001)	3.97	3.96
W(001)	4.08	4.02
W(111)	4.18	3.82

5. Future Work

Precise determination of work functions is required for future detailed investigations of near and sub-threshold photoemission mechanisms in metal photocathodes, such as electron-scattering-mediated Franck-Condon emission.

[1] E.R. Antoniuk et al.; Advanced Materials **33** (2021) 2104081

[2] G. Adhikari et al.; AIP Advances **9** (2019) 065305

Activation Studies for GaAs Photocathodes at Photo-CATCH

Maximilian Herbert[a], Joachim Enders[a], Julian Schulze[a], Markus Engart[a], Maximilian Meier[a], Victor Winter[a] and Vincent Wende[a]

[a]*Institut für Kernphysik, Fachbereich Physik, Technische Universität Darmstadt, Schlossgartenstraße 9, 64289 Darmstadt, Germany*

Abstract

The institute for nuclear physics at TU Darmstadt houses a test stand for Photo-Cathode Activation, Testing and Cleaning using atomic-Hydrogen (Photo-CATCH). It enables dedicated research on, e.g., quantum efficiency and lifetime of GaAs photocathodes as well as DC photo-gun design for future use at the in-house Superconducting Darmstadt Linear Accelerator S-DALINAC. This contribution will give an overview of recent, ongoing and planned activation studies at Photo-CATCH.

1. Photo-CATCH Activation System

1.1. Activation Chamber

The test stand for Photo-Cathode Activation, Test and Cleaning using atomic-Hydrogen Photo-CATCH consists of several XHV chambers for cathode cleaning, activation and operation, including a -60 kV DC gun and a dedicated beamline. The activation chamber features two tungsten coils for heat cleaning of photocathode samples. The activation procedure is carried out using an activation unit, consisting of a ring-anode and two dispensers for Cs and Li, with oxygen being supplied by an external reservoir through a piezo-electric leak valve. The ring-anode is connected to a power supply, providing up to 500 V bias voltage, and the anode current is monitored using an ampere meter. Online pressure measurements are provided using a cold-cathode ionization gauge connected to a gauge controller. All components are connected to an EPICS IOC server.

1.2. Laser System

A laser beam with $\lambda = (785 \pm 5)$ nm and variable laser power is provided by a laser diode placed on an adjacent laser table. An assembly consisting of a half-wave plate, mounted on a motorized precision rotation stage remote-controlled by a DC servo motor controller, and a polarizing beam-splitter is used for PID-based online control of the laser power. The laser beam is transferred to the activation chamber via a fiber optic patch cable. Incident laser power is monitored indirectly by using a non-polarizing beam-splitter cube and a photodiode. Alternatively, an LED array is available, providing illumination of the photocathode with either white or blue light.

1.3. QE Scan Setup

Recently, a setup to measure the quantum efficiency distribution on the photocathode surface has been implemented. A piezo-electrically mounted mirror has been added, enabling to move the laser spot position in a pre-defined grid. An additional non-polarizing beam-splitter an a position-sensitive photodiode was also added for feedback control of the laser spot position, mitigating hysteresis effects of the piezo-electric mount. A sample quantum efficiency distribution measured with the setup is shown in Fig. 1.

2. Activation Studies

2.1. Automated Activation Process

The outcome of the activation process greatly depends on operator input. An automatization of the procedure could simplify and standardize the process. First proof-of-principle tests were carried out at Photo-CATCH[1], yielding promising results. Based on this study, an adaptive algorithm capable of precisely detecting the individual stages of a Co-De process has been developed and successfully tested, yielding results comparable to manual activation[2].

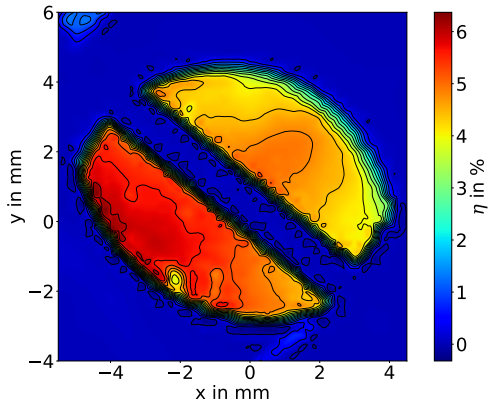

Figure 1. Surface scan of an activated GaAs photocathode in the Photo-CATCH activation chamber. One of the dispensers is blocking part of the view on the photocathode surface. The color bar indicates the measured quantum efficiency η, with each contour line indicating a change in η by 0.3 %.

2.2. Lifetime Enhancement using Lithium

A promising candidate to achieve increased lifetime τ is the addition of Li to an activation with Cs and NF_3 or O_2. A preliminary study at Photo-CATCH[3] yielded a reduction of the quantum efficiency η by a factor of 0.78 ± 0.08, while τ was increased by a factor of 3.5 ± 0.5. The Li-enhanced Co-De scheme devised in this study was improved and used for a direct comparison of Cs+O_2 Co-De with and without Li-enhancement for different doses of Li[4], yielding a significtant increase in τ and lifetime charge $Q(\tau)$ by a factor of 19 ± 2 and 16.5 ± 2.4, respectively, without significant decrease in η.

3. Outlook and Future Work

Additional work on the automated activation process is planned, focusing on on-line control of the amount of introduced oxygen, as well as benchmarking automated versus manual process. Further studies are also planned on Li-enhanced activation in order to optimize the used activation scheme and investigate effects of Li observed during previous studies.

Acknowledgments

The authors acknowledge support by the Deutsche Forschungsgemeinschaft (DFG) - Project ID 264883531 (GRK 2128 “AccelencE”) and the German BMBF (05H18RDRB1).

[1] M. Herbert et al., in Proc. 19th Workshop on Polarized Sources, Targets and Polarimetry - PoS(PSTP2022), Vol. 433, p. 003 (2023).

[2] M. Engart et al., poster at this conference.

[3] N. Kurichiyanil et al., J. Instrum. 14 (8), P08025 (2019).

[4] M. Herbert et al., "Cs-O_2-Li as enhanced NEA surface layer with increased lifetime for GaAs photocathodes", submitted for publication.

A High Intensity Spin-Polarized Electron Photogun to Drive a Polarized Positron Source

C. Hernandez-Garcia[a], M. Bruker[a], J. Grames[a], A. Hofler[a], R. Kazimi[a] and G. Palacios-Serrano[a]

[a] *Thomas Jefferson National Accelerator Facility, Newport News, VA 23606*

1. Abstract

A photogun to generate a high-intensity, highly spin-polarized electron beam > 90 % with unprecedented charge lifetime in the kilocoulomb range is envisioned at JLab for a proposed Ce+BAF polarized positron beam source. The electron photogun is expected to provide a CW beam of > 1 mA for a month without intervention. A limiting factor is ion-back bombardment on the strained-superlattice GaAs-photocathode which can be reduced by improving the photogun vacuum or biasing the anode. Additionally, increasing the laser spot size can help mitigate ion-induced damage. However, eventually the laser size becomes too large for the photogun electrode. An envisioned photogun design will incorporate larger electrodes to accommodate larger and off-center laser spot sizes. Compatible larger conical insulators which operate > 300 kV for beam injection into a $\beta \sim 1$ SRF booster are also necessary.

2. Motivation

The Continuous Electron Beam Accelerator Facility (CEBAF) at Jefferson Lab provides continuous-wave (CW) spin-polarized electron beams with energies up to 12 GeV for nuclear physics experiments[1]. The electron source is based on spin-polarized photoemission using strained superlattice GaAs/GaAsP photocathodes in a 200 kV dc-high voltage photo emission electron gun (photogun). Jefferson Lab is exploring a CEBAF enhancement to also provide spin polarized positron beams for nuclear physics with intensities of ∼ 100 nA[2].

The production of the spin-polarized positron beams is based on the two-step conversion of spin-polarized electrons to polarized bremsstrahlung photons and then to polarized electron/positron pairs in a high-Z solid target. This highly efficient transfer of spin polarization was demonstrated at CEBAF previously successfully demonstrating production of spin-polarized positron beams[3]. The present concept relies on a relatively low energy ∼ 100 MeV, yet high power > 100 kW spin polarized electron beam, consequently the spin polarized photogun is expected to provide > 1 mA continuously for prolonged periods.

3. Introduction

A photogun providing 1 mA of photocurrent will generate 86 Coulombs (C) in a day, 600 C in a week, and 2,400 C in one month. To be practical for a user program, the photocathode charge lifetime should therefore reliably exceed 1 kC, meaning the photogun should operate for approximately one month without intervention before e.g. interrupting beam delivery to exchange the photocathode or rejuvenate its quantum efficiency. The limiting factor in charge lifetime of an UHV/XHV baked photogun is widely acknowledged to be due to ion back-bombardment where neutral gas molecules (mainly hydrogen) are ionized by the electron beam and accelerated towards the negatively biased photocathode.

The CEBAF UHV photogun with an anode bias of + 1 kV providing currents of 150 – 200 μA and laser RMS diameter ∼ 2 mm has demonstrated a charge lifetime of ∼ 0.4 kC[4]. This achievment means the CEBAF photogun would provide 1 mA beam for about one week, which is less than a value of 1 kC needed for the positron program.

4. Experimental Approach

Reducing ion-bombardment is a multi-pronged approach. Improving vacuum conditions in the photogun or adjacent beamline is the best approach. Baked stainless steel hydrogen outgassing rates provide UHV vacuum levels, however, recent studies at Jefferson Lab suggest that utilizing low-carbon steel for the photogun vacuum chamber and electrodes could reduce the outgassing rate by one order of magnitude[5]. Ions originating downstream can enter the photogun and add to ion-bombardment, however, applying a positive bias to the anode can eliminate this contribution and is now used at all of the Jefferson Lab load-lock photoguns[4,5]. Short of eliminating ions, spreading the back-bombardment damage area on the photocathode has shown improvements in lifetime at mA current levels[6]. Record level charge lifetime for a spin-polarized beam were achieved this way[7], but photocathode lifetime appeared to be ultimately limited by the cathode electrode (active area) size – as the laser spot size approaches the exposed diameter of the photocathode. The numerical tracking code IONATOR based on the commercial software General Particle Tracer was developed to predict ion-bombardment. Preliminary simulations of ion-bombardment reproduce the observed distribution of quantum efficiency degradation observed in the CEBAF photogun[8]. This approach may be used to design future electrodes with larger exposed photocathode surface in addition to shifting the drive laser wavelength a few nm from the bandgap energy[9].

5. Outlook and Future Work

A JLab Laboratory Directed Research and Development award was recently granted to support a two-year project at our Gun Test Stand to systematically explore and optimize the laser size/position and cathode/anode electrodes to increase charge lifetime. The resulting photogun is envisioned to be eventually moved into the Low Energy Recirculator Facility to provide high power beams for testing positron production targets.

Aside from reducing ion-bombardment a major technical challenge lies in raising the breakdown voltage of inverted-geometry insulators to reliably achieve 400 – 500 kV in order to efficiently inject into SRF cavities following the photogun. This voltage is unprecedented for inverted-geometry insulators we prefer. Utilizing a 0.45 m long inverted-insulator developed in 2010 we recently demonstrated that commercial cable components are capable of achieving 500 kV[10] . The proof of principle relied on adapting a rigid epoxy commercial cable receptacle to the inverted-insulator by means of an intervening SF_6 volume. To prevent arcing in inverted-geometry insulators and commercial epoxy receptacles connected to high-voltage cables, it is essential to displace all air between the cable rubber connector and the rigid receptacle or insulator. Since there is no rubber cable connector fitting the large available insulators, a rigid epoxy receptacle was shaped to the conical contour of the insulator, and in place of the flexible rubber, a 1 cm gap was left between the insulator and the modified receptacle. The resulting 2-liter volume was then evacuated and backfilled with SF_6. Encouraging results will be published in a peer-reviewed journal.

6. Acknowledgments

This work was produced in part by Jefferson Science Associates, LLC under Contract No. AC05-06OR23177 with the U.S. Department of Energy. Publisher acknowledges the U.S. Government license and provide public access under the DOE Public Access Plan.

[1] P. A. Adderley *et al.*; Phys. Rev. Accel. Beams **27**, 084802 (2024)
[2] J. Grames *et al.*; https://doi.org/10.48550/arXiv.2309.15581
[3] D. Abbott *et al.*; Phys. Rev. Lett. **116**, 214801 (2016)
[4] J. Yoskowitz *et al.*; Phys. Rev. Accel. Beams **27**, 123401 (2024)
[5] A. Al-Allaq *et al.*; AVS 70th International Symposium & Exhibition, Nov. 3–8, 2024
[6] J. Grames *et al.*; Phys. Rev. ST Accel. Beams **14**, 043501 (2011)
[7] J. Grames *et al.*; Proceedings of Science (**324**) PSTP2017
[8] M. Bruker *et al.*; Proc. IPAC '24, MOPC52, 176–179
[9] E. Wang *et al.*; Appl. Phys. Lett. **124**, 254101 (2024)
[10] Hernandez-Garcia *et al.*; Proc. NAPAC 2022, WEPA16, 651–654

Cathodes with Optimized QE for Driving a Polarized e^+ Source

Kurt Aulenbacher[a], **Monika Dehn**[a], **Werner Lauth**[a] **and Jennifer Trieb**[a]

[a]*Institut für Kernphysik der Johannes Gutenberg-Universität Mainz*

1. Abstract

Polarized positron beams generated from 10-100 MeV-class accelerators may become useful for applied physics and also for high energy physics. The intensity of the driving polarized electron source is one of the most important limiting factors for the positron beam intensity. Since the absorbed laser power may exceed several Watt, quantum efficiency and heat transfer of the photocathode need to be optimized. Resonance enhanced GaAs/GaAsP superlattices will be expedient to solve these challenges. We also discuss how the availability of such complicated heterostructures could be improved.

2. Introduction

Polarized positrons can be produced by a double conversion process from a polarized electron beam. Such a beam has for instance been realized at the MAMI facility in Mainz [1] where a 530 MeV beam of positrons is available which is produced from the 855 MeV electron beam. The principle of operation is illustrated in figure 1. The transverse normalized emittance is about $20\mu m$ (geometrical emittance at 530 MeV is estimated as $0.014\,mm \cdot mrad$), and the energy width is of the order of several percent.

When using the polarized electron beam of MAMI with its typical polarization of 85% , a spin-transfer to the positrons can be expected, as it was demonstrated at JLAB [2]. Hence a high quality and, if needed, polarized positron beam is available at 530 MeV. However, the conversion efficiency is only $\approx 2 \cdot 10^{-8}$, mostly because of the thin ($10\mu m$) target involved - which reduces Coulomb-scattering and therefore minimizes emittance growth. Operating at lower energy and larger target thickness and with a more sophisticated capturing lens for the positrons, an efficiency of the order 10^{-5} may be obtained as it has been shown by extensive simulations in a study made at IJCLab in Orsay[3]. This, however, is bought by a considerable increase in emittance, the simulations show a geometrical emittance of the order $10mm \cdot mrad$ at 60 MeV. In any case, to achieve a reasonable brightness for experiments in applied and particle physics, high current spin-polarized **electron** beams with average currents in the range of 1 mA are needed [4]. In the following we present the implications for the photocathode properties.

3. Quantum efficiency and heat transfer

Presently, spin-polarized sources use GaAs-based heterostructures, mostly GaAs/GaAsP superlattices which can be fabricated with typical thicknesses of about 10% of an absorption length, i.e. only 10% of the available light intensity can be absorbed. Losses at the interfaces then limit quantum efficiency (QE) to about 1%. Absorption can be resonantly increased by using a distributed Bragg reflector (DBR) at the backside of the (front side illuminated) cathode. Together with the high refractive index of GaAs at the interface with vacuum this forms an etalon with distinct resonances. The multiple reflections do not compromise the polarization significantly. One of the most successful applications of this principle has been achieved by a cooperation of JLAB physicists and a commercial vendor[5]. Quantum efficiencies of $> 6\%$ have been achieved at 780 nm which corresponds to > 35 mA/Watt. Having an operational buffer of 2 lifetimes - taking into account the unavoidable exponential decay of QE - means that at the end of the operation about 200-300 mW of laser power will be absorbed by the structure if one Milliampere has to be sustained.

Recently, our group performed measurements where a GaAs-sample absorbed powers of 2 Watt. The sample was mounted on a Boron-nitride cylinder which enabled application of 30 kV. Boron-nitride is a very good electrical insulator but it offers orders of magnitudes higher thermal conductivity if compared to conventional insulating materials. The increase in cathode temperature was <50 degree at 2 Watt [6]. As rule of thumb, the cathode temperature should not exceed 50 degrees Celsius to avoid a significant shortening of lifetime. This can be guaranteed if the DPR cathode with its few hundred Milliwatt power requirement is used. In consequence, achieving the high QE with the DBR results in a situation where the increase of cathode temperature becomes manageable at current levels exceeding one Milliampere.

4. Generation of low energy spin-polarized positrons

For high energy applications, e.g. colliders for particle physics, it is evident that an accelerator-based source will profit from the reduction of geometric emittance caused by the post-acceleration process. However, for most applied science applications, the energies of positrons must be low. It is well known that polarized positrons can be moderated in matter to energies in the keV range or even lower, if the starting energy is of the order ≈ 1 MeV [7]. To achieve this, the positrons must be decellerated to MeV-scale energies. This will of course lead to an increase of geometrical emittance which has to be taken into account. Another possibility is to make use of the fact that also the positrons at the low energy end of the spectrum profit from the helicity transfer. Here the question is, how such positrons can be extracted from the target and how large the losses associated with multiple scattering will be.

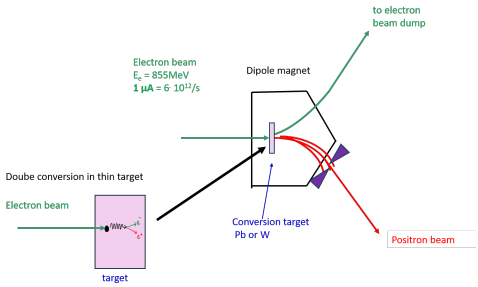

Figure 1. Principle of the Positron source at MAMI.

5. Outlook and Future Work

The commercial availability and sustainable quality of even "ordinary" GaAs/GaAsP-superlattices are of concern. The demand of the photocathode community is not always strong enough to convince vendors to produce the complicated structures. Our group has therefore made contact with the German research institution for applied science, the Fraunhofer-association. A program has been defined to ensure quality control of the structure growth step by step. We hope to start production runs for the GaAs/GaAsP superlattices - starting with the non-DBR structure first - together with the Heinrich Hertz institute of Fraunhofer-association within the next year.

[1] A. Mazzolari *et al.*; https://arxiv.org/abs/2404.08459 (2024)
[2] D. Abbott *et al.*; Phys. Rev. Lett; **116** 214801 (2016)
[3] S. Habet: Concept of a polarized electron source for CEBAF, PhD Thesis, Université Paris-Saclay, CNRS, IJCLab, 91405, Orsay, France. (2023)
[4] M. Bruker *et al.*, in Proc. IPAC2024, MOPC52, DOI:10.18429/JACoW-IPAC2024-MOPC52", (2024)
[5] W. Liu *et al.*: Appl. Phys. Lett. **109**, 252104 (2016)
[6] M.Dehn *et al.*: Proceedings IPAC 15, Nashville, TN, doi: 10.18429/JACoW-IPAC2024-WEPC53 (2024)
[7] J. van House *et al.* Phys. Rev. A **29,1** 96–105 (1984)

DBR photocathodes for EIC polarized electron source

Omer Rahman[a]

[a]*Brookhaven National Lab, Upton, NY, USA*

1. Abstract

Distributed Bragg Reflector (DBR) GaAs photocathodes were tested in high voltage DC gun at BNL with operating voltage up to 300 kV. Several methods were implemented to mitigate the surface charge limit and up to 11.6 nC (in 1.6 ns bunch) was obtained.

2. Challenges for Polarized Electron Source for EIC

The Electron Ion Collider (EIC) at Brookhaven National Lab (BNL) requires a polarized electron source capable of delivering 7 nC of polarized electrons with polarization higher than 86%. The bunch length from the gun is 1.6 ns which makes extracting such high charge a challenging problem. To mitigate this problem, we used a high surface layer dopant density (5×10^{19} atoms.cm^{-3}) DBR Strained Superlattice GaAs photocathode in a high voltage DC gun with 300 kV voltage. The level of voltage and the required vacuum level for acceptable lifetime made this gun a challenging problem.

3. DBR Photocathode

The DBR SSL GaAs was Fabricated at Old Dominion university and tested at BNL [1,2]. The cathodes were grown using Metal-Organic Chemical Vapor Deposition (MOCVD) method. The DBR layer is composed of 12 pairs of $GaAs_{0.65}$ $P_{0.35}$ and $In_{0.30}$ $Al_{0.70}P$ with nominal thicknesses of 54 nm and 64 nm, respectively, and p-type Zn doping of 5×10^{18} cm^{-3}. No protective As cap was deposited on the cathode. The cathodes were tested at mini-mott polarimeter at BNL for ESP and QE. Then they were used in the gun for the bunch charge and lifetime measurement. Surface layer is carbon doped with an optimal dopant density of 5×10^{19} atoms.cm^{-3} .

During the characterization phase of these photocathodes, we found that that with increasing dopant density, the polarization decreases. We also found that from sample to sample and from activation to activation on a single sample, the peak QE wavelength can change as much as 20 nm. The easiest solution to the changing peak QE wavelength was to implement a wavelength tunable laser.

4. The EIC Polarized Electron Gun

The EIC polarized electron gun is a high voltage DC (HVDC) gun. The ceramic is inverted style and the gun was high voltage commissioned up to 350 kV. The operational voltage for this gun is 300 kV with a test beam line capable of measuring bunch charge and lifetime, as shown in figure 1.

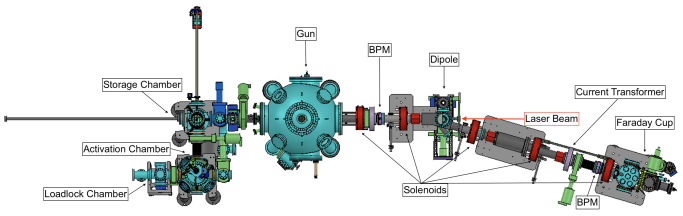

Figure 1. The EIC polarized electron gun and the test beamline

5. Suppressing the Surface Charge Limit

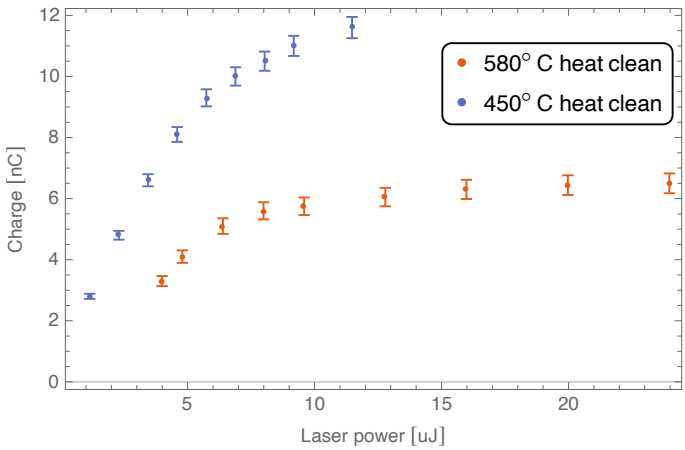

Figure 2. Dependency of heat cleaning temperature on the extracted bunch charge

Higher doping level on the surface layer of SSL GaAs has been implemented at SLAC to mitigate surface charge limit. For our surface doping level of 5×10^{19} atoms.cm^{-3}, the peak polarization was measured to be 90%. Any higher doping level would result in polarization level lower than 80%. During the cathode preparation, we tried the traditional 580 ° celcius heat cleaning of the DBR sample before activation. During this run, we found that the extracted charge starts to saturate around 5.5 nC, even after increasing the voltage to 320 kV and increasing the laser spot size. We suspected that the high heat cleaning temperature is diffusing the surface dopant and decreasing the effective doping level to suppress surface charge limit. We employed a lower temperature 450 °C heat clean and found that we could extract as high as 11.6 nC charge. Therefore, it was proven that a lower temperature heat clean can help with preserving the high dopant density on the surface layer of the DBR cathode. We also tried increasing the laser spot size for even higher charge and found that extracted charge does not scale linearly with increasing spot size. This indicates that surface charge limit needs to be treated as a 3D problem, instead of the traditional 1D problem.

6. Lifetime Measurements

We measured the lifetime from the DBR photocathodes with 7.5 nC bunch charge and 30 μA average current. We found that that charge lifetime has wavelength dependency. Lifetime for wavelength higher than the peak QE wavelength is substantially lower compared to wavelength lower than the peak QE wavelength.

7. Outlook and Future Work

We propose to treat Surface charge limit as a 3D problem instead of the traditional 1D model. To mitigate surface charge limit, we also propose to use gradient doping on the surface of the cathode instead of uniform doping on the surface. In this way doping concentration is constant under the laser spot, then increases radially outward. We are in the process of building a HV test stand to perform surface charge limit experiments on various cathode in the future.

[1] B. Belfore; Appl. Phys. Lett. 2023; **123** (22)
[2] E. Wang; Appl. Phys. Lett. 2024; **124** (25)

HELMHOLTZ ZENTRUM
DRESDEN ROSSENDORF

Bautzner Landstr. 400
01328 Dresden, Germany
Phone +49 351 260-3548
Fax +49 351 260-13458
Email r.xiang@hzdr.de
http://www.hzdr.de